TURBULENCE MEASUREMENTS IN THE WALL JET LAYER OF AN IMPINGING ROUND JET

A Thesis Submitted to
the Graduate School of Engineering and Science of
İzmir Institute of Technology
in Partial Fullfillment of the Requirements for the Degree of

MASTER OF SCIENCE

in Mechanical Engineering

by
Serdar MALAK

July 2012
İZMİR

We approve the thesis of **Serdar MALAK**

Examining Committee Members:

Assist. Prof. Dr. Ünver ÖZKOL
Department of Mechanical Engineering
İzmir Institute of Technology

Assoc. Prof. Dr. Moghtada MOBEDİ
Department of Mechanical Engineering
İzmir Institute of Technology

Assoc. Prof. Dr. Serhan KÜÇÜKA
Department of Mechanical Engineering
Dokuz Eylül University

4 July 2012

Assist. Prof. Dr. Ünver ÖZKOL
Supervisor, Department of Mechanical Engineering
İzmir Institute of Technology

Prof. Dr. Metin TANOĞLU
Head of the Department of
Mechanical Engineering

Prof. Dr. R. Tuğrul SENGER
Dean of the Graduate School of
Engineering and Sciences

ACKNOWLEDGMENTS

I would like to express my sincere gratitude to my supervisor Assist. Prof. Dr. Ünver ÖZKOL for his enlightening advises and guidance through the thesis.

Fluid Mechanics Laboratory members, especially Orçun KOR have great contribution during my experimental studies. Their encouraging commendations and helps motivated me so much when I faced difficulties.

Lastly, I would like to thank to my lovely family. They have always encouraged and supported me, and they were always patient even in my darkest hours.

ABSTRACT

TURBULENCE MEASUREMENTS IN THE WALL JET LAYER OF AN IMPINGING ROUND JET

The objective of this thesis is to understand how turbulence affects the impinging jet flow and heat transfer mechanism under acoustic actuaion. This work is based upon the experimental work including velocity and turbulence measurements in various cases and is a continuation of studies of Necati Bilgin and Orcun Kor . Acoustic actuation is provided by a loudspeaker controlled by a function generator. Acoustic waves generated by the loudspeaker reaches nozzle and formed periodic fluctuations in flow. Strouhal number, which is dimensionless reperentation of actuation frequeny, is varied in the range of $0<St<1$. Nozzle exit velocity is controlled by Reynolds number whics is kept constant around 10000. Velocity and turbulence measurements were performed by using a hot-wire sensor. Measurements are performed in the radial direction ranging from the jet centerline (x/D=0) to 2.4D for jet profile data and to 8.5D for near wall data. Wall normal measurement locations are at z/D=5.8, 5, 4, 3, 2, 1, 0.2 for jet profile data and at z/D=5.8 for near wall data. The distance between data points is kept at 0.1D.

ÖZET

BİR YÜZEYE ÇARPAN DAİRESEL KESİTLİ JET AKIŞININ DUVAR JETİ BÖLGESİNDEKİ TÜRBÜLANS ÖLÇÜMLERİ

Bu tezin amacı, yüzeye çarpan bir jet akışının akustik titreşimler altında, türbülansın akış karakterisriklerini ve ısı transferi mekanizmasını nasıl etkilediğini anlamaktır. Bu çalışma, çeşitli durumlarda hız ve türbülans ölçümlerini içeren deneylere dayanmakta ve Necati Bilgin ve Orçun Kor'un çalışmalarının devamı niteliğindedir. Akustik uyarı, bir fonksiyon üretecinin kontrolündeki bir hoparlörle sağlanmıştır. Hoparlör tarafından oluşturulan akustik dalgalar lüleye ulaşıp akışta periyodik çalkantılar oluşturmaktadır. Uyarı frekansının birimsiz hali olan Strouhal sayısı 0 ile 1 arasında değiştirilmiştir. Lüle çıkış hızı, 10000 civarında tutulan Reynolds sayısı ile kontrol edilmiştir. Hız ve türbülans ölçümleri sıcak-tel duyargasıyla yapılmıştır. Ölçümler, radyal yönde; jet profili verisi için jet merkezinden 2.4D ve duvara yakın bölge verileri için 8.5D mesafeye kadar yapılmıştır. Duvara dik yöndeki ölçümler jet profili için z/D=5.8, 5, 4, 3, 2, 1, 0.2; duvara yakın bölge için z/D=5.8 mesafelerinden ölçülmüştür. Ölçüm noktaları arasındaki mesafe 0.1D kadardır.

TABLE OF CONTENTS

LIST OF FIGURES

Figure **Page**

LIST OF TABLES

Table **Page**

LIST OF SYMBOLS

D	Jet diameter	m
f	Actuation frequency	1/s
Tu	Turbulence intensity	
Nu	Nusselt number	
Re	Reynolds number	
St	Strouhal number	
U	Instantaneous velocity	m/s
u'	Fluctuating velocity	m/s
u'_{rms}	Root mean square of fluctuating velocity	m/s
u	Uncertainty	
x	Radial distance of the jet	m
X	Radial direction coordinate	
z	Axial distance of the jet	m
Z	Axial direction coordinate	
$\dot{\forall}$	Volumetric flow rate	m^3/s

Greek letters

ν	Kinematic viscosity	m^2/s

Subscript

c	centerline
Rms	Root mean square
mean	Mean

CHAPTER 1

INTRODUCTION

Jet impingement is a known technique of achieving high heat transfer coefficients. Therefore it is widely used in many engineering applications such as cooling of materials, electronic equipment, and critical machining surfaces, turbine blades, drying of paper or textile products, processing of steel or glass.

As compared to the other techniques, it can be seen that fluid is used more efficiently in jet impingement, because impingement boundary layers are much thinner than parallel flow boundary layers. Zuckerman and Lior. (2005) report that given a required heat transfer coefficient, the flow required from an impinging jet device may be two orders of magnitude smaller than that required for a cooling approach using a free wall-parallel flow. A typical boundary layer for jet impingement and parallel flow is illustrated in Figure 1.1

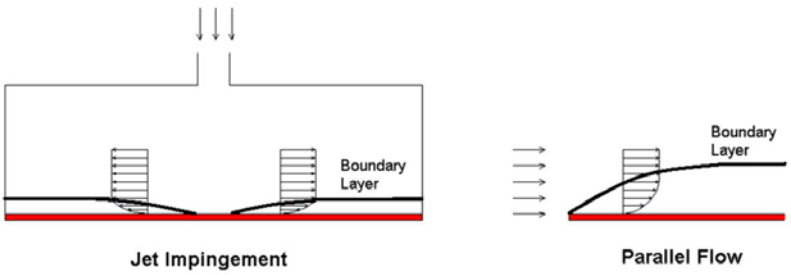

Figure 1.1. Comparison between boundary layer of jet impingement and parallel flow (Source: Bilgin 2009)

1.1. Types of Jet Impingement

Impinging jets can be divided in to two main groups as liquid jets and gas jets by the type of working fluid. It also can be classified into five groups by a hydrodynamic point of view: free-surface, plunging, confined and wall jets Wolf et al. (1993). This classification depends on how the flow interacts with the surface and the ambient fluid, as schematized in Figure 1.2. For the free-surface jet is, liquid is injected to an immiscible atmosphere and the liquid travels nearly without mixing into the

impingement plate. The plunging jet impinges into a pool of which surface is covered by a liquid, where the depth of the pool is less than the nozzle-to-surface spacing. The submerged jet is injected into a miscible atmosphere. The confined jet is injected into a section which is bounded by the impingement surface a nozzle plate. The wall-jet flows parallel to the surface.

A combination of confined and a submerged type jet is used for this study. These kinds of jets are chosen for compact and efficient electronic cooling applications because of their suitability.

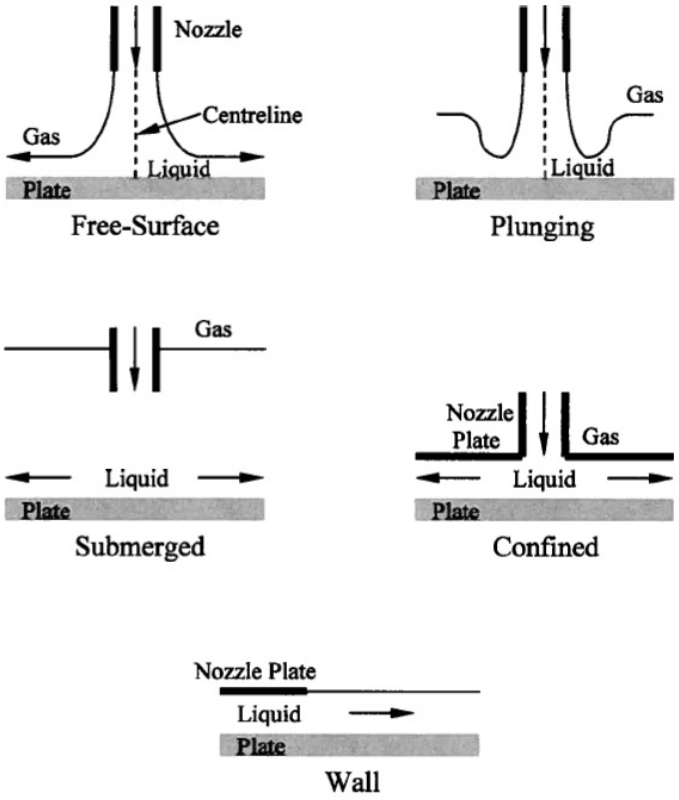

Figure 1.2. Different types of jet impingement
(Source: Franco 2008)

Jets can be divided into two groups from the aspect of flow regime: Laminar or turbulent jets. Zuckerman and Lior (2005) suggested that the flow field behaves laminar at Re < 1000 and turbulent at Re > 3000. A transition region occurs between these two regimes.

A classification can be made by the number of jet nozzles: single jets and multi jets (jet arrays). The jets can also be classified with respect to its shape such as circular, rectangular or slot jets.

1.2. Hydrodynamics of Jet Impingement

There are three major factors of the hydrodynamics of the jet flow. These are the initial flow state, the type of the stationary ambient fluid and the location of the impinging plate with respect to the nozzle.

The jet is generally turbulent at the nozzle exit and is represented by a uniform velocity profile. Starting of its development stage, the jet is surrounded by a mixing layer, but in the center it has irrotational flow. Increasing distance from nozzle exit, momentum exchange, which causes free boundary layer of the jet to broaden and the potential core to contracted, occurs between the jet and the surrounding fluid. During the jet's flow, velocity profile becomes non-uniform and the centerline velocity decreases at the downstream from the nozzle exit.

Deflection zone is where the jet decelerates in axial direction but starts to accelerate in radial direction. Fluid velocity continues to increase until it reaches the speed of the jet flow in radial direction (Franco 2008), then the fluid behaves as it's in parallel flow, which it traverses parallel to the surface without further acceleration.

The jet impingement which occurs orthogonally on a plane surface is commonly divided into four zones (Figure 1.3).

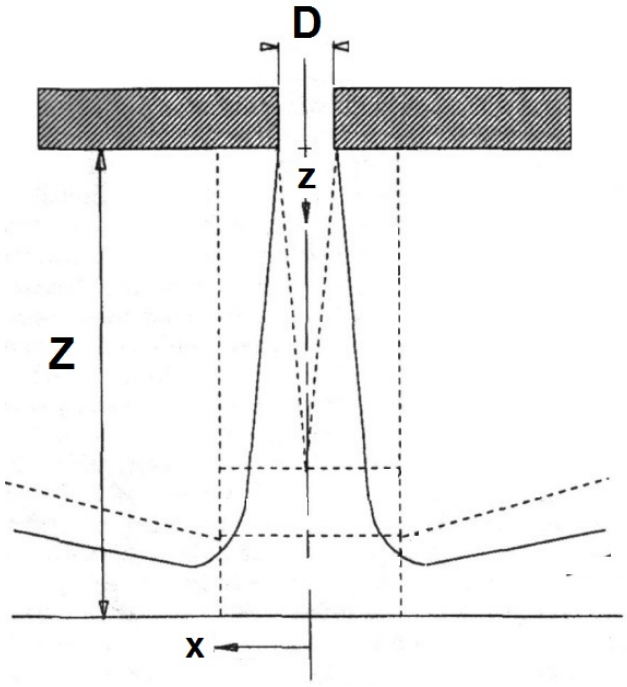

Figure 1.3. Flow zones of an impinging jet: Zone 1, initial mixing region; zone 2, established jet; zone 3, deflection zone; zone 4, wall jet (Source: Jambunathan et al. 1992)

A definition which is shed light on the key points of impinging jet flow has been suggested by Jambunathan et al. (1992) as it is shown below:

(1) There is a developing flow zone where fluid from the surroundings is entrained into the jet, thus reducing the jet velocity. This region is called as mixing or shear region which surrounds a core region. The core region is where fluid velocity at the centerline of the jet (U_c) is almost equal to the nozzle exit velocity (U_{inlet}) and is often called as potential core. A common end of the core region is the point where $U_m = 0.95U_{inlet}$.

(2) At greater nozzle to plate spacing the axial velocities reduce with increasing distance from the nozzle exit. Schlichting (1968) showed that the fall of the centerline velocity and the jet half width will be directly proportional to the axial distance from the end of the potential core.

(3) The near plate region is often named as deflection zone. Axial velocity rapidly reduces and a corresponding rise occurs in static pressure in that region. Jambunathan et al (1992) report that, the measurements of Tani and Komatsu (1966) had shown, aforementioned region extends approximately two nozzle diameters from the plate surface for air jets.

(4) Flow changes its direction and goes parallel to the wall when impinges to the plate surface. This is the region called wall jet zone. Within this region, radial velocity rises rapidly and after a while decays as goes by in radial direction from stagnation point.

1.3. Jet Parameters

The characteristic of an impinging jet is depended on various parameters, which can be dimensional or non-dimensional.

The dimensional parameters are nozzle diameter (D), and jet exit velocity (U_{inlet}), and nozzle-to-plate spacing (D).

Non-dimensional parameter can be count as Reynolds number ($\mathrm{Re} = U_{inlet} D / \nu$), non-dimensional nozzle-to-plate spacing (Z/D).

Nozzle geometry, flow confinement, initial turbulence intensity also affects the characteristic of jet.

For acoustically actuated jet; various parameters such as actuator's position, actuation amplitude, frequency (f) and waveform are thought to be important parameters. When frequency is involved, one can use a non-dimensional parameter called Strouhal number ($St = fD/U_{inlet}$).

1.4. Definition of Wall Jet

A wall jet was defined as a shear flow directed along the wall where, by virtue of the initially supplied momentum, at any station, the streamwise velocity over some region within the shear flow exceeds that in the external stream by Launder and Rodi (1979). This definition is very comprehensive and many flows or phenomena can be investigated under this consideration.

In the scope of this work, a radial wall jet which is formed by an impinging round jet is studied.

1.5. Hot-Wire Anemometry

Hot-wire and hot-film anemometers are defined as "devices used to measure the variables occurring in turbulent flows, such as mean and fluctuating velocity components, mean and fluctuating temperature, etc." by Comte-Bellot (1976). Thermal anemometry is usually used when rapidly varying velocities is needed to be measure with good spatial and time resolution.

Probes can be found in various types, and generally formed from basic parts as sensor, prongs, and probe support. An illustration of a hot-wire probe is shown in Figure 1.4. Hot-wire sensors are typically 0.5-5μm in diameter and 0,1-1mm in length. Tungsten and platinum is most used materials of sensors. Sensors are made of very thin metallic elements, and heated by electric current. Therefore the sensor is cooled by convecting fluid flow. Anemometer circuitry keeps the temperature on the sensor constant; therefore this cooling event gives chance to measure quantities in the flow.

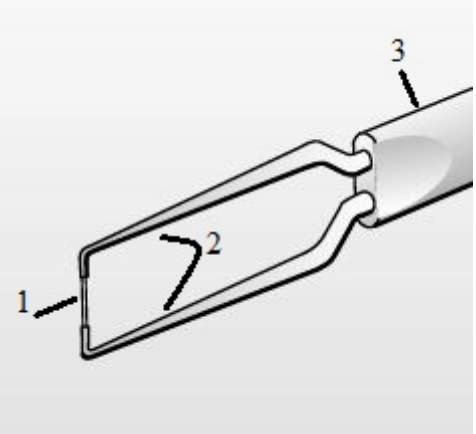

Figure 1.4: An example hot-wire: 1, sensor; 2, prongs; 3, probe support
(Source: Dantec Hot-Wire Catalog)

1.6. Motivation

Many jet impingement applications aim to achieve high heat transfer coefficients, and literature survey detailed below points out that obtaining aimed results depends on geometry of surroundings, turbulence intensity of jet and nozzle-to-plate spacing. Manipulating these parameters by various techniques is commonly used.

The objective of this thesis is to investigate how the turbulence characteristics affect the impinging jet under acoustic actuation.

CHAPTER 2

LITERATURE SURVEY

Many studies have been conducted on convection cooling with jet impingement technique especially for last a few decades due to the need for higher cooling rates in various industrial fields such as electronics, steel production or in energy. This chapter is prepared to give brief information about literature written on the related subjects which are connected to the scope of this work.

Due to the large number of different applications, the literature has been limited to the studies concerning about round confined jets. Velocity and turbulence measurements, their effects on heat transfer characteristics are reviewed.

2.1. Effects of Nozzle-to-Plate Spacing

Nozzle-to-plate spacing is axial distance between nozzle exit and impingement plate. This parameter affects turbulence intensity and heat transfer rate at stagnation point and in radial direction.

The axial variations of velocity and turbulence were investigated by Gardon and Akfirat (1965). They showed that, turbulence intensity in a free jet could reach up to 30 percent of nozzle exit velocity at nearly 8 nozzle diameters downstream. Similarly, Schlunder and Gnielinski (1967) point out that both maximum turbulence and maximum stagnation point heat transfer occur at Z/D=7.5.

The radial variation of heat transfer coefficient is also investigated by Gardon and Carbonpue (1962) and reported that three peaks (x/D=0.5, 1.4 and 2.5) were observed. These peaks are explained as follows.

First peak at x/D=0.5 is explained as the change in the radial velocity which is in the direction from end of the stagnation region to the wall-jet region. Second maxima at x/D=1.4 is explained by a transition from laminar to turbulent boundary layer flow. Third maxima at x/D=2.5 where toroidal vortices which form in the shear region around circumference of the jet impinge to the plate (Popiel and Trass, 1982).

Knowles and Myszko (1998) showed that nozzle-to-plate spacing has a large effect on the peak level of turbulence, in the radial direction up to x/D~4.5. Initial wall jet thickness is also found dependent the nozzle-to-plate distance in the same work.

O'Donovan and Murray (2007) studied jet impingement heat transfer and published their results in two companion papers. Their results has shown that at low nozzle to surface spacings (<2 diameters) secondary peaks in the radial heat transfer distributions are due to an abrupt increase in turbulence in the wall jet. In particular the velocity fluctuations normal to the impingement surface have a controlling influence on the enhancement in the wall jet.

Roux et al. (2011) investigated the flow and heat transfer of an impinging jet under acoustic excitation experimentally. They concluded that acoustic forcing modify the flow structure, creating annular vortex rings in the shear layer of the jet, considered as coherent structures. Pairing phenomenon takes place in the jet for higher and non-natural Strouhal number forcing. This acoustic forcing has not a strong effect on the heat transfer for Z/D = 5, because the vortices stay far enough from the plate. However for Z/D = 3, the forcing can modify the Nusselt number distributions. The secondary peak, which is clearly detected without forcing, is shifted and alleviated with acoustic forcing. The location of this peak seems to be linked to the position of the maximum turbulence level close to the plate.

Nozzle-to-plate spacing is chosen as 6 diameters in this study. The experimental set-up of this study is mainly differs from literature as it is not listed in Wolf's categorization mentioned in the first chapter.

2.2. Effects of Reynolds Number on Jet Flow

Many researchers have been studied on Reynolds number effects on heat transfer of an impinging jet.

Turbulence has large benefits on enhancing heat transfer. Martin (1977) showed behavior of flow at various Reynolds numbers, for instance, at Re<1000 the flow field shows laminar flow properties whereas at Re>3000 the flow has turbulent.

O'Donovan and Murray (2007) has given the Nusselt number distribution in radial direction on impingement surface. It can be seen from their results that, heat transfer is greater for higher Reynolds numbers. They also concluded that secondary

peaks in heat transfer rates increases by increasing nozzle-to-plate spacing. However, the highest peaks are dependent Reynolds number.

2.3. Effects of Confinement on Jet Flow

Another parameter that affects impinging jet flow is confinement. A schematic view of unconfined jet, confined jet, and present study is shown in Figure 2.1. Submerged jet is an unconfined jet and directly injected into a miscible atmosphere. Confined jet is injected into a section which is bounded by the impingement surface a nozzle plate. For this study, a combination of submerged and confined jet is used.

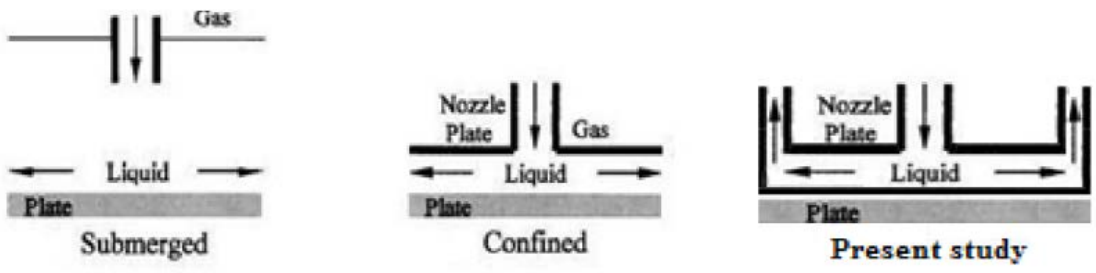

Figure 2.1. Schematic comparison of unconfined jet, confined jet and present study

Obot et al (1982) showed that there is reduction, which increases with increasing the flow rate, in the heat transfer caused by confinement.

Baydar and Ozmen (2005) investigated flow structures of unconfined and confined impinging air jets. Their study shows that, turbulence intensity along the impingement surface has two distinct peaks for both unconfined and confined jet configurations. The first peaks occur in in the same locations for both cases, whereas the second peak for unconfined jet is closer to the stagnation with respect to the confined jet. They concluded that, there is a linkage between the peaks in turbulence intensity and heat transfer coefficients in the impingement plate.

2.4. Effects of Turbulence Intensity on Jet Flow

Measured values in turbulent flow are instantaneous that means vary in time. These variations have irregular fluctuations about mean values. Instantaneous values

give rise to difficulties while using them in calculations, thus they have to be decomposed in to simpler forms. Reynolds decomposition is one of these decomposition methods which is given in (2.1) lets one to decompose any instantaneous value into a time averaged (a.k.a. mean) and a fluctuating part. Temperature and pressure values can also be decomposed similarly.

$$U = U_{mean} + u' \tag{2.1}$$

The turbulence intensity is defined as

$$Tu = \frac{u'_{rms}}{U_{mean}} \tag{2.2}$$

where u'_{rms} is the root mean square of fluctuating velocity component and $\overline{U}$ is the mean velocity component. Similarly, intensity values for other coordinates can be defined.

The effects of small scale turbulence on heat transfer in impinging jet are investigated by Den Oueden and Hoogendoorn (1974). They showed that turbulence intensity at the nozzle exit has an impact on heat transfer at the stagnation point for a certain nozzle-to-plate spacing (Z/D=2). However, the results of Gardon and Akfirat (1965) showed that, initial turbulence level is relatively small for Z/D=6, because generated turbulence in the shear layer predominates the initial turbulence. Hoogendorn (1977) also found that for nozzle-to-plate spacing larger than 5 diameters, Nusselt number profiles had a peak directly under the jet axis.

Large scale turbulent flow structures in the free jet highly affect transfer coefficients in the stagnation region and wall jet region. The vortices formed in the free jet-shearing layer, categorized as primary vortices, may penetrate into the boundary layer and exchange fluids of differing kinetic energy and temperature (or concentration). The ability of the primary vortex to dynamically scrub away the boundary layer as it travels against and along the wall increases the local heat and mass transfer (Zuckerman and Lior, 2006).

Turbulent flow along the wall may also cause additional vortices also known as secondary vortices. Turbulent fluctuations in radial velocity can produce local flow reversals along the wall. This formation is shown in Figure 2.2. Chung and Luo (2002) studied a numerical analysis of an unsteady impinging jet. They concluded that large-

scale vortex activity along the wall may generate a secondary peak in transfer coefficients and causes most of the variation in Nusselt number over time.

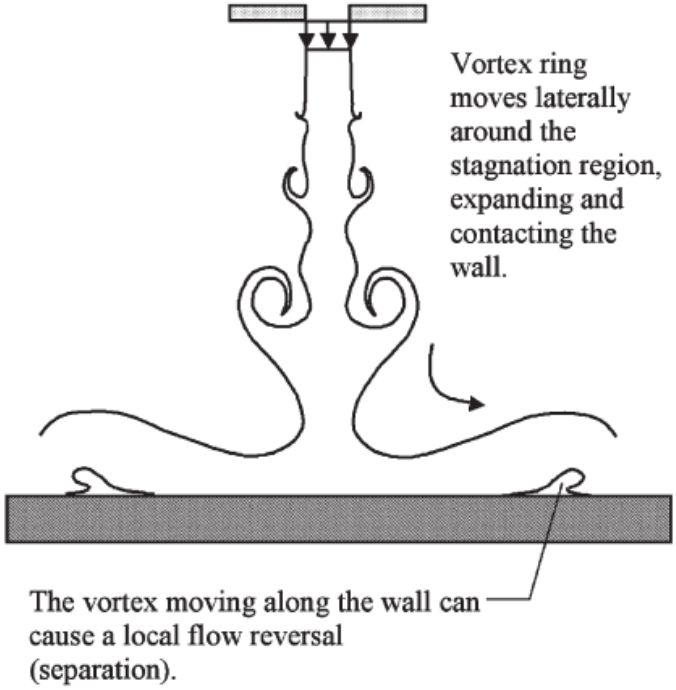

Figure 2.2. Vortex motion in the impinging jet
(Source:Zuckerman and Lior, 2006)

2.5. Jet Actuation

Researchers used actuated jets firstly to determine the sources of the noise in the jet. Later on, the possible effect of actuation on characteristics of jets was understood. The method could be used to control the large and small scale motions of jets, thus attention on jet actuation grown accordingly.

Wiltse and Glezer (1998) studied on direct excitation of small scale motion in free shear flow. Their study was conducted for Re=17800. They concluded their study as “excitation leads to enhanced transfer of energy from the large scales to the small scales”.

Hussain and Zaman (1981) studied turbulence suppression in free shear flows for Re=21400. They noted that phase-locked coherent structures couldn’t be measured beyond six diameters downstream of nozzle exit. Moreover, they reported that, turbulence intensity in the actuated and non-actuated jets is also the same between six and eight diameters along z-direction.

Raman et al. (1989) studied effect of initial turbulence on jet's evolution for Re=610000. Their work showed that, initial turbulence intensity is relevant to respond of jet to the excitation. They found that, jets which have turbulence intensities varied from 0.15 to 0.5 percent responded to the excitation. They also suggested that the amplitude of excitation is increased with increasing initial turbulence intensity.

Hwang and Cho (2003) studied on effects of acoustic excitation positions on heat transfer under condition of Re=34000. They reported that for St=1.2, heat transfer rates enhanced a little at small nozzle-to-plate spacing, due to the high turbulence intensity. However, that rate reduces at larger spacing, because of the lower stream velocity.

CHAPTER 3

EXPERIMENTAL SET-UP

3.1. Jet Parameters of Experimental Set-up

A jet impinging set-up, which was built to investigate the effects of nozzle geometry nozzle-to-plate spacing, radial distance from the jet centerline and frequency and waveform of actuation, is used in this study. The set-up was first built by Bilgin (2009) and some changes was made by Kor (2010). This work has been continued up to their design and recommendation about the future works.

Fundamental dimensions were decided based on impinging jet parameters. These parameters are non-dimensional radial distance from jet centerline (x/D), non-dimensional axial distance from nozzle exit to impingement plate (Z/D), Reynolds and Strouhal numbers. A detailed view of jet zones and axes are given in Figure 1.3.

Jet diameter is chosen as 5 mm in order to have a spatial resolution of the jet and keep the side boundary conditions relatively far away. Nozzle-to-plate spacing is chosen as 6 diameters. Reynolds number is kept constant at 10000 in the entire investigation. Investigated Strouhal numbers are 0 (no actuation case), 0.175 and 1. In Figure 3.1 section view of test section is shown.

3.2. Working Principles of the Experimental Set-up

This work contains series of experiments with a combination of confined and submerged jet. These types of jets have an effective heat transfer performance mostly in compact design of cooling.

A standpipe is used to adjust the flow coming to test section. A honeycomb is located at the downstream end of the standpipe. It is used to suppress the swirl motion in the flow before nozzle entrance. The working fluid is left test room through the gap between the standpipe and the test room. The gap is 3 mm wide. The fluid is sent back to supply tank.

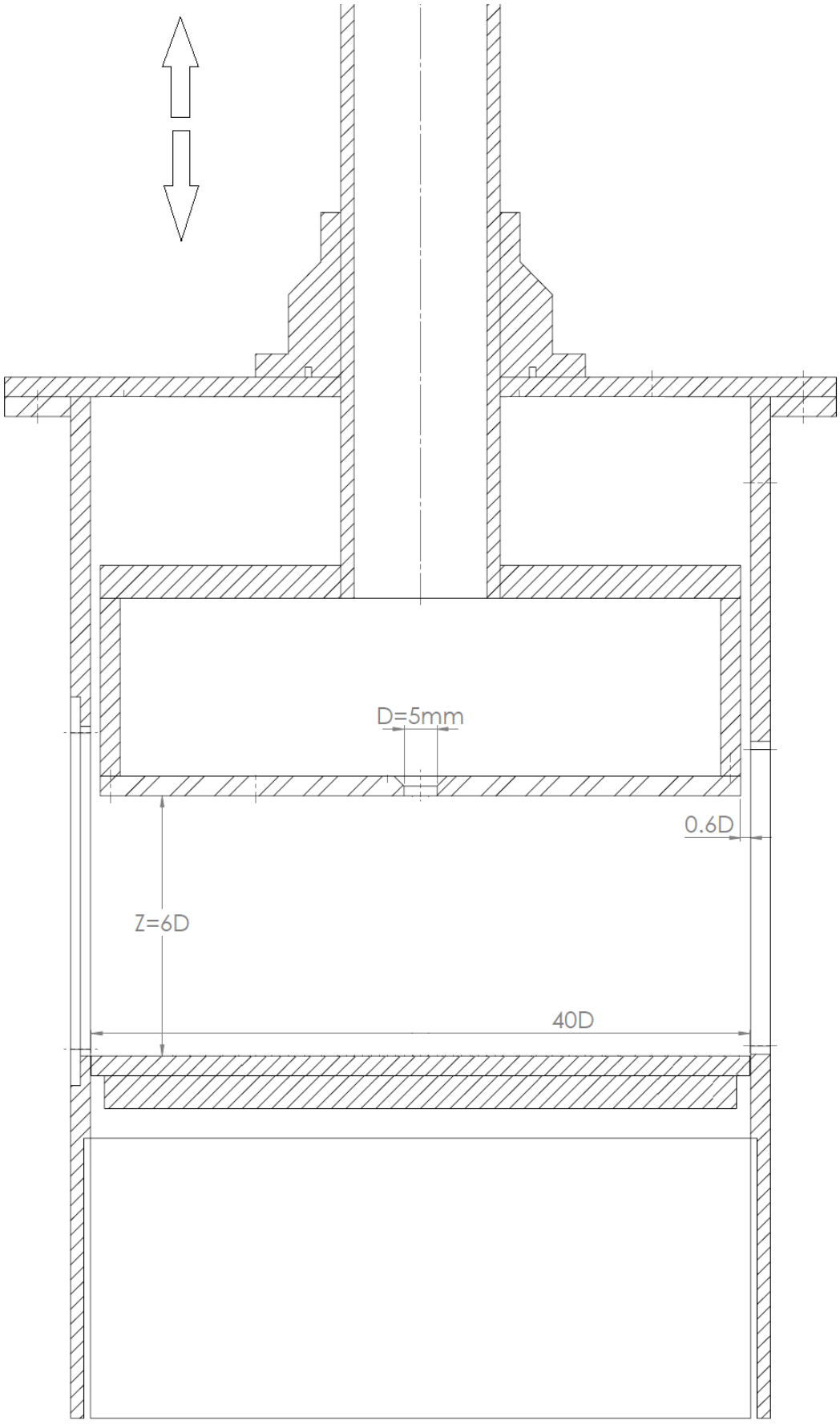

Figure 3.1. Section view of test section

3.3. Water Jet Experiments

Water is used as working fluid in all experiments. A schematic view of experimental setup is shown in Figure 3.2.

Water collected in the water tank (4) provided the jet velocity of 2 m/s by means of free fall. Constant jet velocity is stabilized by controlling the height of free surface of water at a certain level. The water tank supplied from supply tank (1) by a diaphragm pump (2).

The flow diagram can be described as follow: Water taken from supply tank is transferred to pump by supplying pump line (i) and pumped to the water tank through supplying water tank line (ii). Water tank supplies the jet set-up through the line (iii). Water is actuated by sound waves which are created by loudspeaker (5), and then actuated water impinges to the plate. Used water is taken away to the drainage through line (iv).

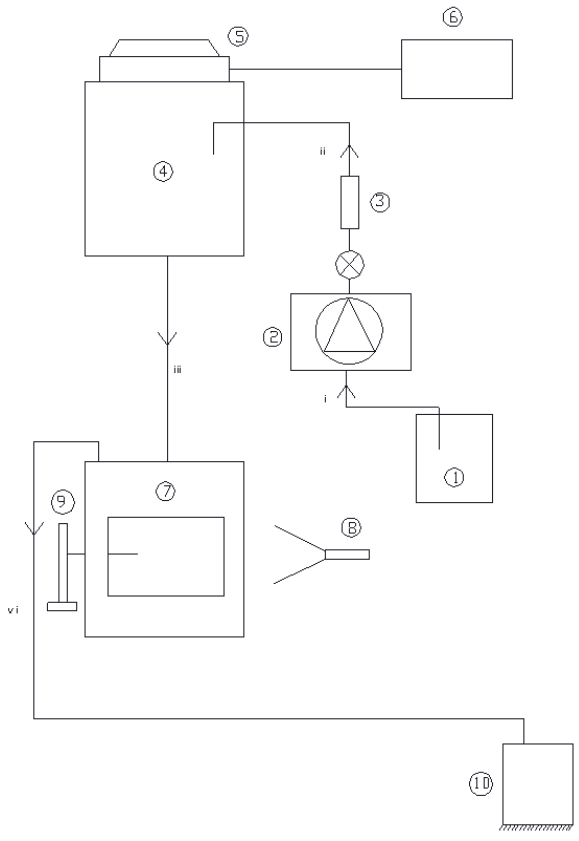

1. Supply tank
2. Pump
3. Flow meter
4. Water tank
5. Loudspeaker
6. Amplifier
7. Jet setup
8. Laser
9. Hot-wire and traverse mechanism
10. Drainage

i. Supplying pump line
ii. Supplying water tank line
iii. Jet supplying system line (in)
iv. Jet supplying system line (out)

Figure 3.2 . Experimental set-up for water jet

A laser (8) is used to illuminate the jet room while preparing the location of the hot-wire probe. The traverse mechanism (9) stands to move the hot-wire probe at wall normal and radial directions.

The supply tank contains clean water for the experiments. The height of the water in the water tank was watched carefully and observed that it is steady.

The loudspeaker is mounted on the water tank. It is 11 inches in diameter and 450 W in acoustic power. Working range of the loudspeaker is between 25 Hz and 2500 Hz. It is controlled by an amplifier which is fed by sinusoidal waves generated by a function generator.

The general view of test section and travers mechanism is given in Figure 3.3.

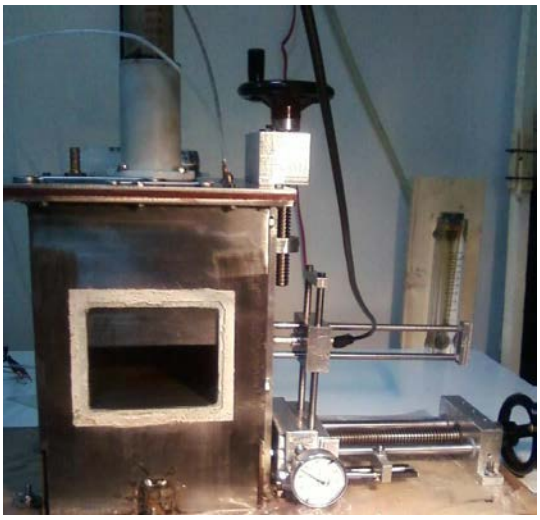

Figure 3.3. General view of test section and traverse mechanism

Turbulence measurements conducted using TSI 1276-10AW hot-film sensor attached to the TSI IFA-300 model constant temperature anemometer. Hot film sensor (Figure 3.4) has dimensions which 0.25mm in active length and 0.0254mm in diameter. Maximum operation temperature of hot film sensor is 67 degrees Celsius.

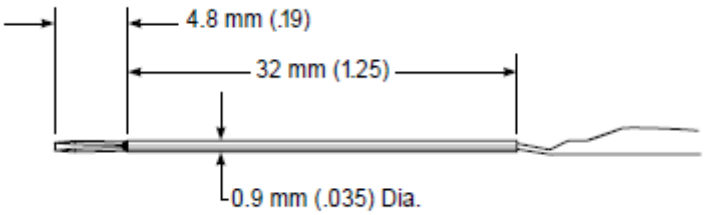

Figure 3.4. Illustrative view of hot film sensor (a detailed view is given in Figure 1.4)

The data is acquired at 10 kHz sample rate and for approximately 6.55 seconds. The range of measurements are performed in the radial direction ranging from the jet centerline (x/D=0) to 2.4D for jet profile data and to 8.5D for near wall data. Wall normal measurement locations are at z/D=0.2, 1, 2, 3, 4, 5, 5.8 for jet profile data and at z/D=5.8 for near wall data. The distance between data points is 0.1D. Measurement layers in axial direction and boundaries in radial direction are shown schematically in Figure 3.5.

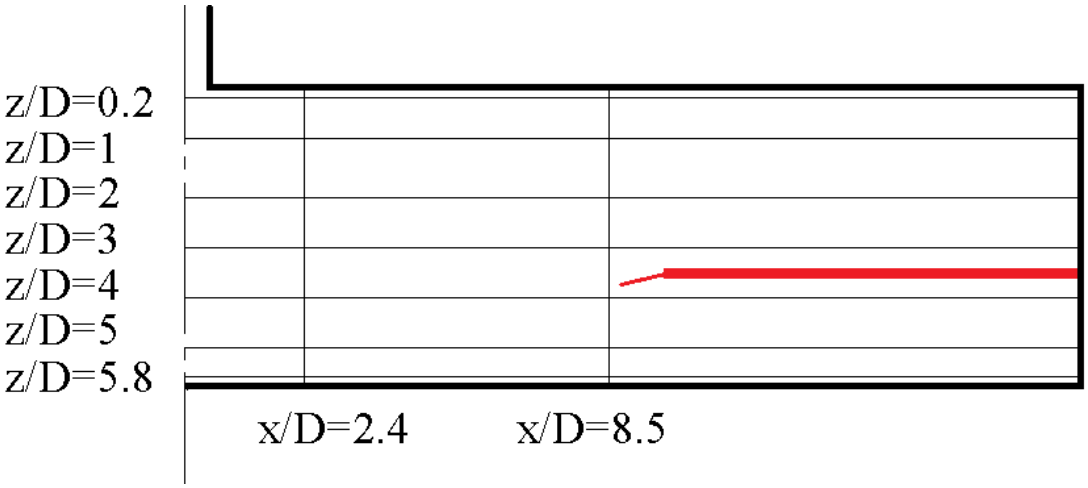

Figure 3.5. Hot-wire measurement layers and boundaries

Hot-wire is positioned at the center of test section. Movements have been achieved by controlling the traverse mechanism along axial and radial directions. Before acquiring data, hot-wire calibrated at the nozzle exit. Since nozzle exit velocity could be obtained by the help of continuity equation, center of the nozzle exit is chosen as the calibration point. The hot-wire sensor is calibrated at the same point before each set of experiments (e.g. jet profile measurements or wall-jet measurements). Thus, two different calibration curves are given in Figure 3.6.

Measurements show resultant velocity values rather than only one direction. This drawback is due to using single wire sensor. For instance, axial component of velocity vector reaches its maximum value at jet centerline, but as it can be understood from velocity plots in this study, there is some points where velocity value is its maximum at radial positions differ from the jet centerline. However, the dominant component of velocity vector can be easily assumed by considering the physics of flow. It is clear that axial component is dominant at nozzle exit as radial component is dominant at wall-jet region.

Acquired data preprocessed using Thermal Pro software which is bundled with anemometer and then these preprocessed data is analyzed with self-written MATLAB code. MATLAB code basically takes instantaneous velocity data and compute mean and fluctuating velocity values. The turbulence intensity is calculated using the root-mean-square of the fluctuating velocity values at each data point divided by mean velocity value. The root mean square is defined as follows:

$$x_{rms} = \sqrt{\frac{1}{n}({x_1}^2 + {x_2}^2 + ... + {x_n}^2)} \tag{3.1}$$

where x is a measured quantity and n is number of data.

(a)

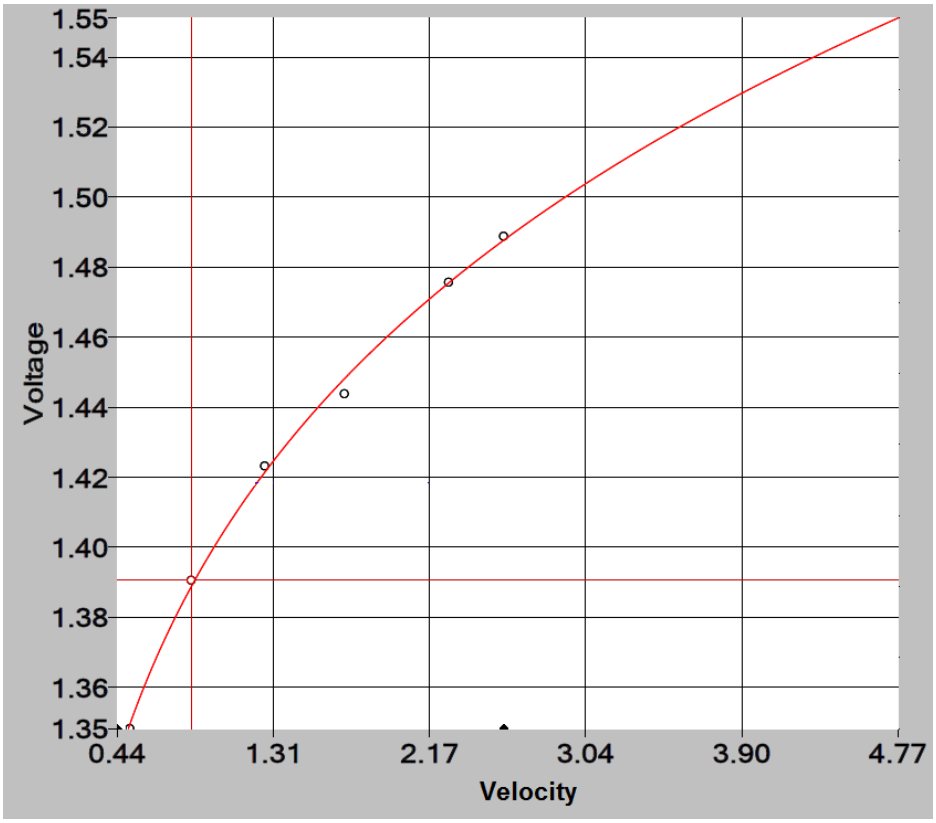

(b)

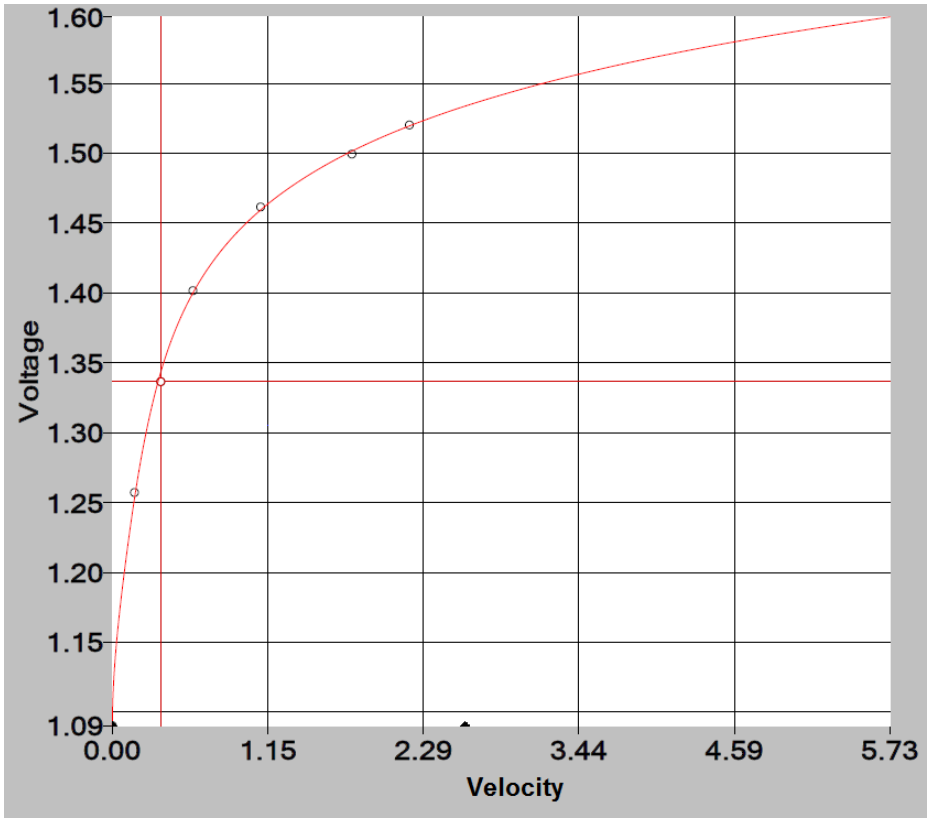

Figure 3.6. Calibration curves: (a) for jet profile measurements; (b) for wall-jet region measurements

CHAPTER 4

RESULTS AND DISCUSSION

4.1 Uncertainty Analysis of Experimental Data

Experimental works always have errors. Errors are inevitable but there is an interval where these errors are acceptable. The interval is defined by uncertainty analysis. The term uncertainty is used to refer to "a possible value that an error may have.", and this definition is expressed by Kline and McClintock (1953). Since the results of experiments are used for engineering analysis and design, uncertainty analysis helps us to validate data.

For a given R function of x_1, x_2, …, x_n, uncertainty is defined as

$$u_{R_i} = \frac{x_i}{R}\frac{\partial R}{\partial x_i}u_{x_i} \tag{4.1}$$

where u_{R_i} is the uncertainty in R function, x_i is the measured value, ∂x_i is the accuracy of measurement, ∂R is the variation in R, and the u_{x_i} is the uncertainty in measured data. When combined effects are needed to calculate, all x_i's should be taken into account; Hence, Kline and McClintock (1953) suggested a representation of uncertainty equation that includes all errors:

$$u_R = \pm\left[\left(\frac{x_1}{R}\frac{\partial R}{\partial x_1}u_1\right)^2 + \left(\frac{x_2}{R}\frac{\partial R}{\partial x_2}u_2\right)^2 + \ldots\left(\frac{x_n}{R}\frac{\partial R}{\partial x_n}u_n\right)^2\right]^{1/2} \tag{4.2}$$

Results of uncertainty analysis are tabulated in Table 4.1.

Table 4.1. Experimental uncertainties

Quantity	Percentage uncertainty (%)
$\dot{\forall}$, volumetric flow rate (*l/min*)	± 3.45
Re, Reynolds number	± 3.60
U, velocity *(m/s)*	± 2.00

4.2. Velocity and Turbulence Intensity Measurements

Hot-wire measurements are taken from locations given in Chapter 3.3. Figure 4.1 shows normalized velocity profiles for three different actuation cases (no actuation; St=0, actuated; St=0.175 and St=1). Normalization is done by using the jet centerline velocities which are given in legends of the plot. When plots are examined, it can be seen that some maximum velocity values are located outside from jet symmetry axis. This situation is already explained as measurements show resultant values in Chapter 3.3. When Figure 4.1 is examined, it is seen that the jet has been thickening just after the nozzle exit (z/D=0.2). However, it has been getting narrow at next layer which is z/D=1, and thickening again at following layers. This difference is thought to be an unexpected. It is presumed that, entrainment flow from confinement plate to the jet makes a contribution to the radial component of velocity vector at nozzle exit; therefore this initial thickening might be an error due to using a single wire sensor.

When velocity profiles at z/D=5.8 are examined, the points that the maximum velocity value is measured moves away from the jet centerline. In addition to this, an increase in velocity with increasing Strouhal numbers is seen. The reason for this is thought to be toroidal vortices which formed around the jet and which affected from actuation vibrations. If flow field is measured by particle image velocimetry (PIV), fact lying behind this occurrence might be proved.

The plot for St=0.175, the velocity profile at z/D=4 layer differs from the other in shape. This difference is thought to be a result of roll-up event that will be shown in Figure 4.2.

St=0

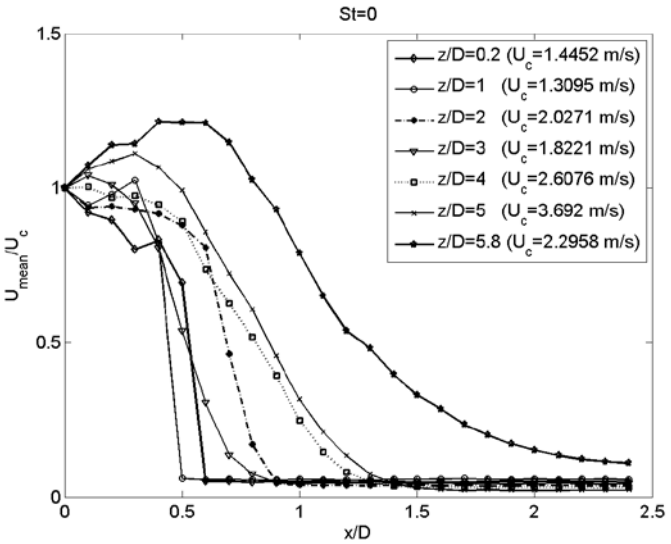

St=0.175

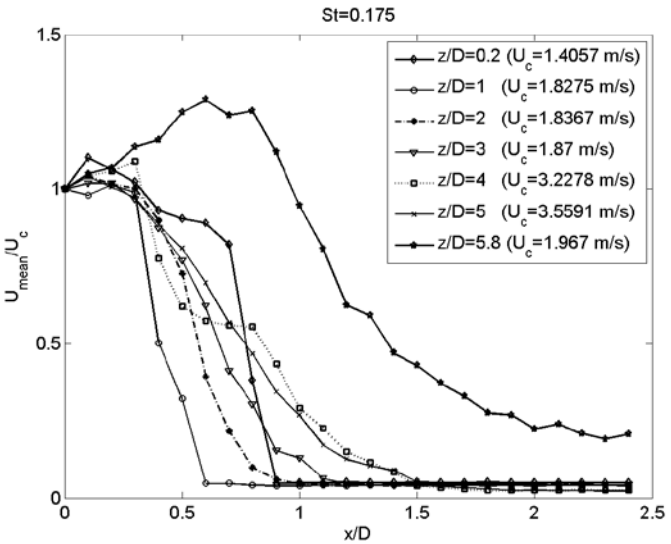

St=1

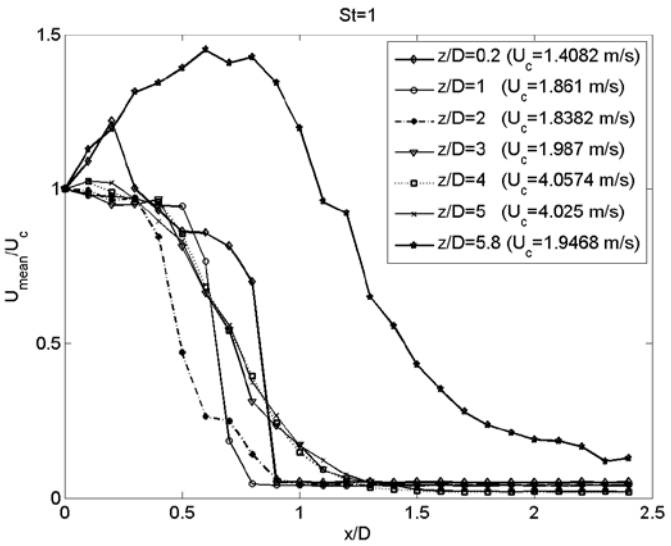

Figure 4.1. Mean velocity profiles for three different St numbers

Normalized mean velocity and turbulence intensity profiles is given for three different actuation case and seven different layers (z/D=0.2, 1, 2, 3, 4, 5, 5.8) separately in Figure 4.3-Figure 4.9.

It is seen from velocity profiles that radial velocities originated from confinement plate towards the jet increase with increasing Strouhal numbers at z/D=0.2 layer (Figure 4.3). It is understood that, the situation is due to acoustic actuation. Similarly, turbulence intensity is getting wide at the same location. The highest intensity is obtained for St=0.175 case. Frequency related to St=0.175 is thought that it creates a special unsteady situation. Additionally, roll-up event is observed at that frequency. Flow visualization images of this event are shown in Figure 4.2.

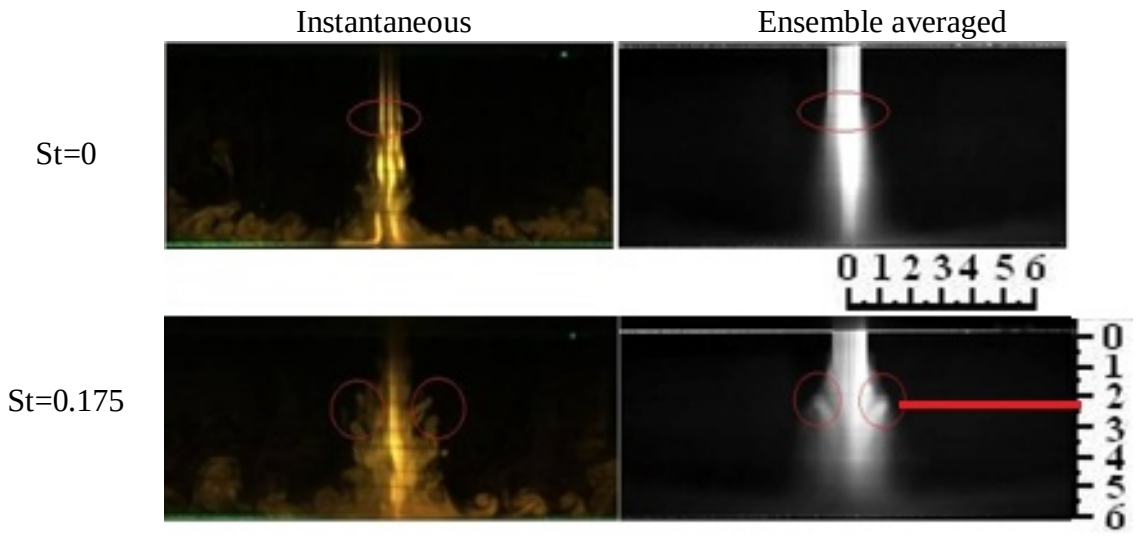

Figure 4.2. Instantaneous vs. ensemble averaged images
(Source: Kor, 2010)

As seen in Figure 4.4, the turbulence intensity at shear layer of the jet is measured higher for St=0.175 and 1 compared to the no actuation case. The increase in the turbulence intensity at shear layer is not observed for St=0. A possible reason is thought that radial velocity at the nozzle exit might be relatively small in magnitude. The effect of shear layer on turbulence intensity is clearly seen at layer corresponding to z/D=2 and 3.

An interesting circumstance related with roll-up event is observed at z/D=4 layer. When St=0.175 case is considered, it is seen that turbulence values reach levels much higher compared other samples at the same layer. The reason for this could be originated from two sources: Firstly, turbulence at the shear layer of the jet could be

transferred to the jet center by vortices growing with the roll-up event. Secondly, generation of turbulence at the jet center due to deformation of velocity profile.

The layers at z/D=5 and 5.8 have similar characteristics because of their closeness to the stagnation point, thus, they could be commented together. The turbulence intensities at these layers are seen to be dependent on diffusion in radial direction. Moreover, the turbulence intensities at the jet centerline are increased and have a profile with two maxima. This kind of profiles is seen for all three actuation cases. However, as it might be predicted, the highest turbulence intensity is obtained at the case of St=0.175 with a percentage of 35%.

St=0

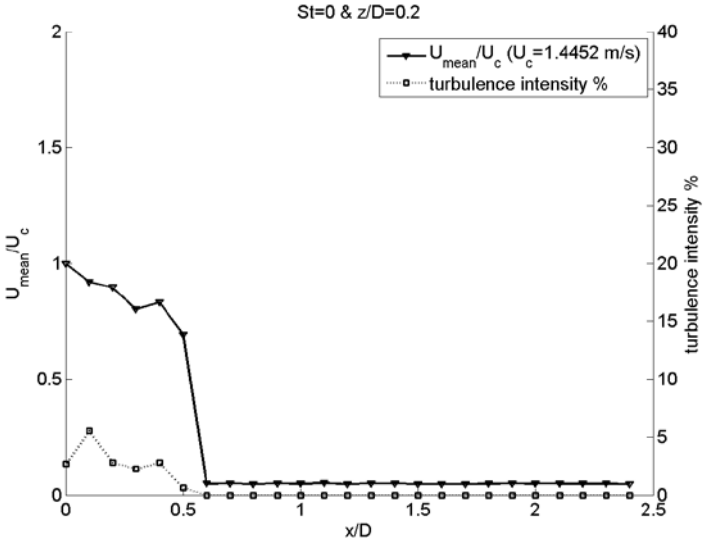

St=0.175

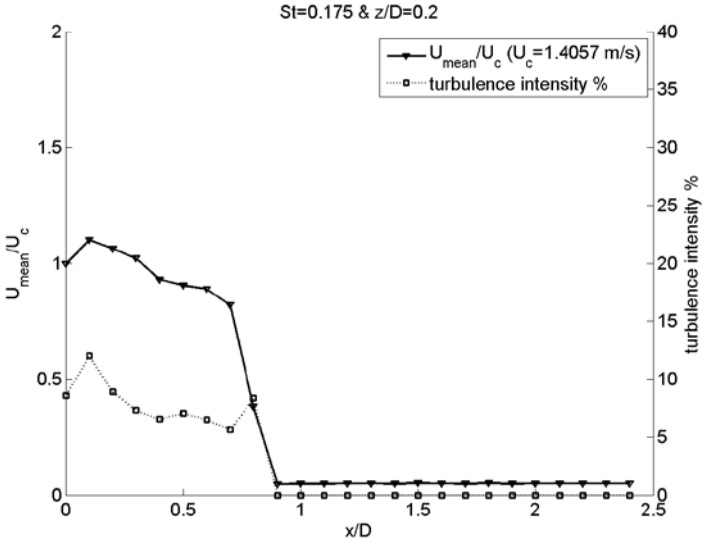

St=1

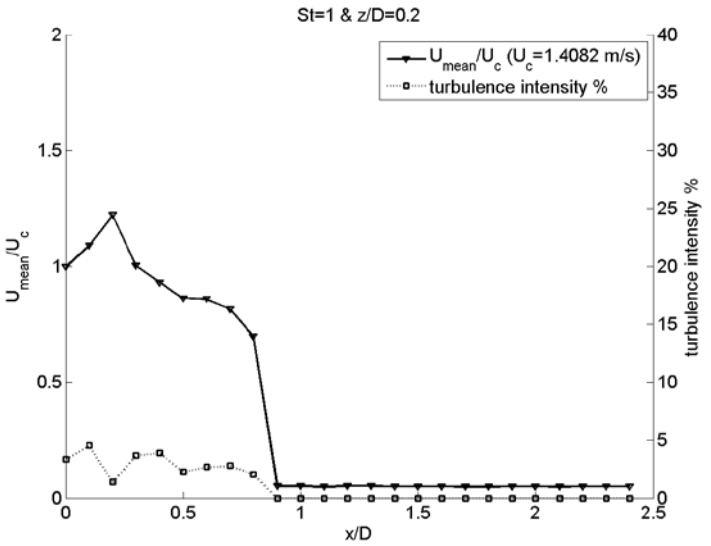

Figure 4.3. Normalized mean velocity and turbulence intensity plots for z/D=0.2

St=0

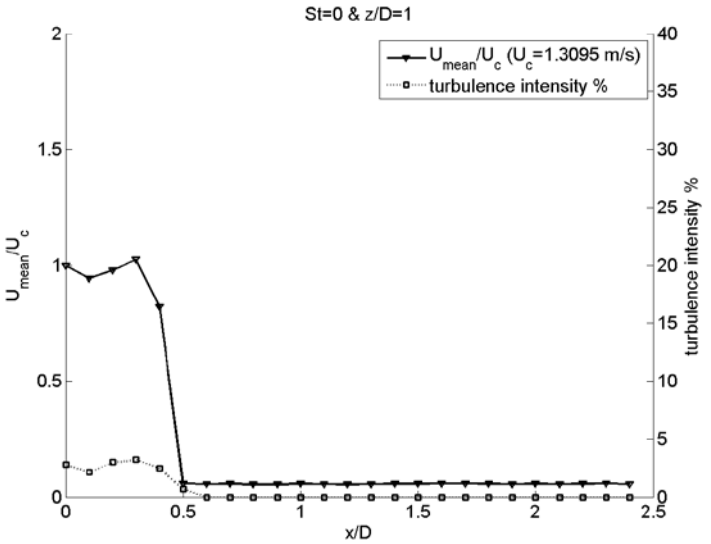

St=0.175

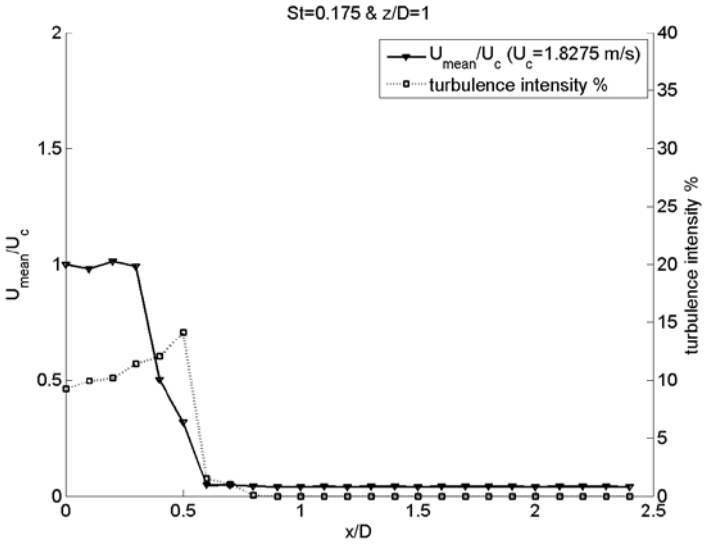

St=1

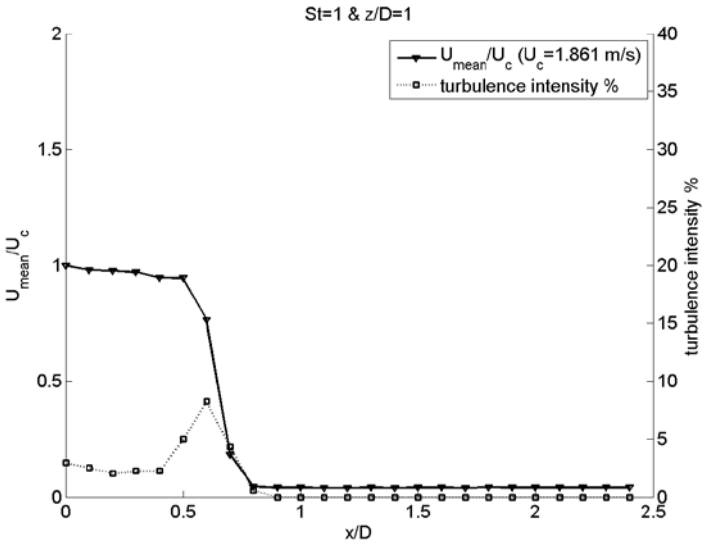

Figure 4.4. Normalized mean velocity and turbulence intensity plots for z/D=1

St=0

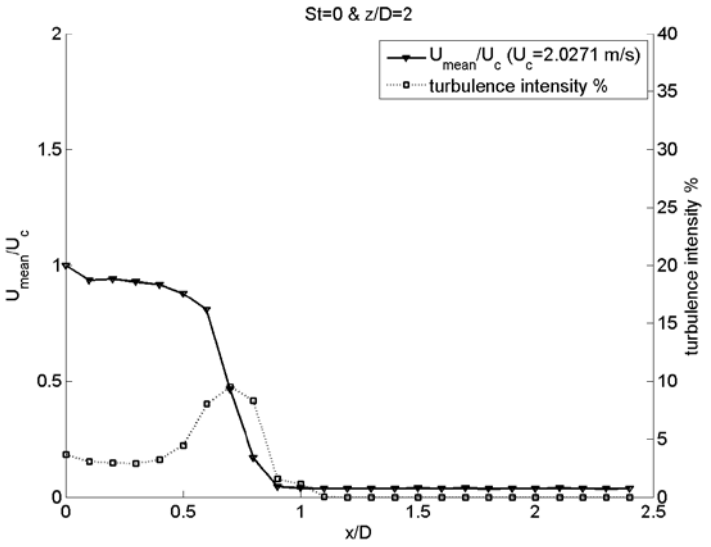

St=0.175

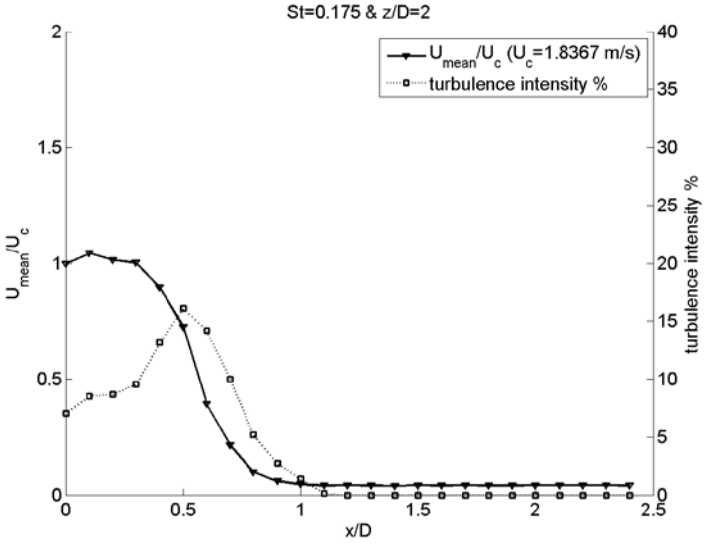

St=1

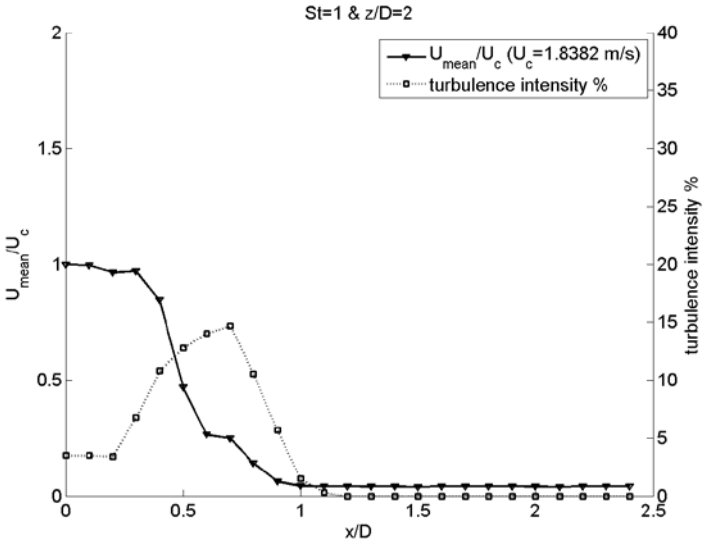

Figure 4.5. Normalized mean velocity and turbulence intensity plots for z/D=2

St=0

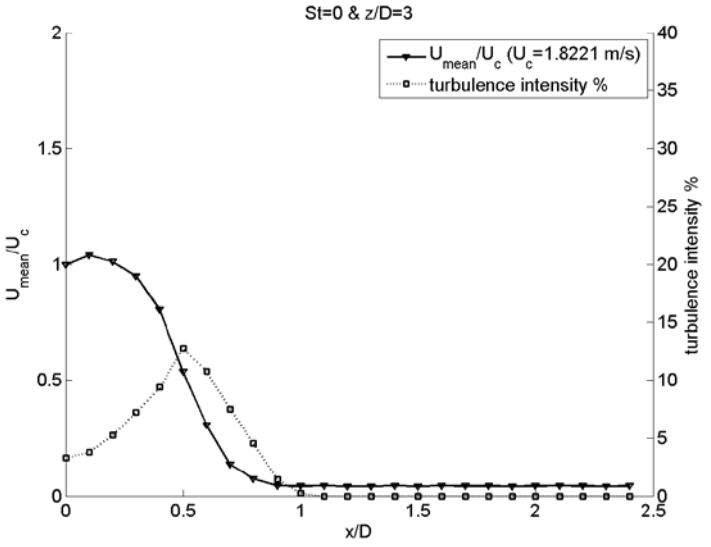

St=0.175

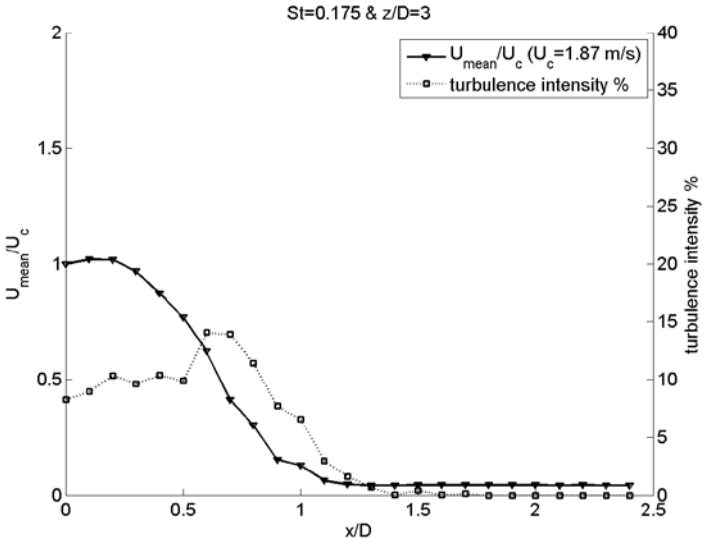

St=1

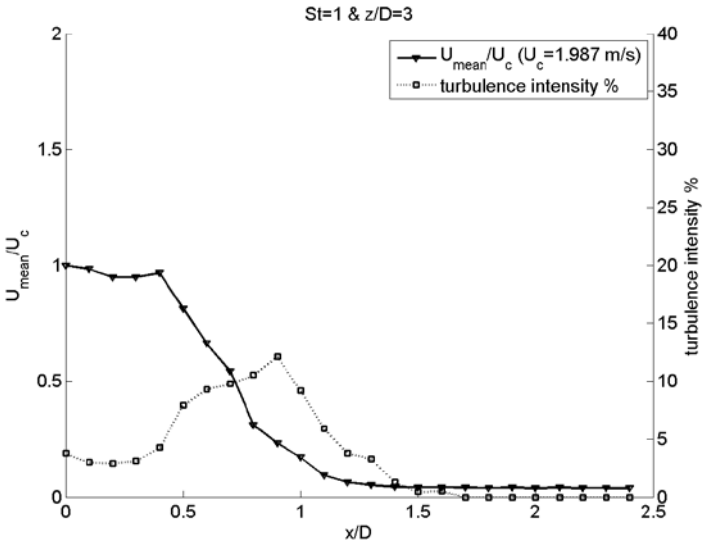

Figure 4.6. Normalized mean velocity and turbulence intensity plots for z/D=3

St=0

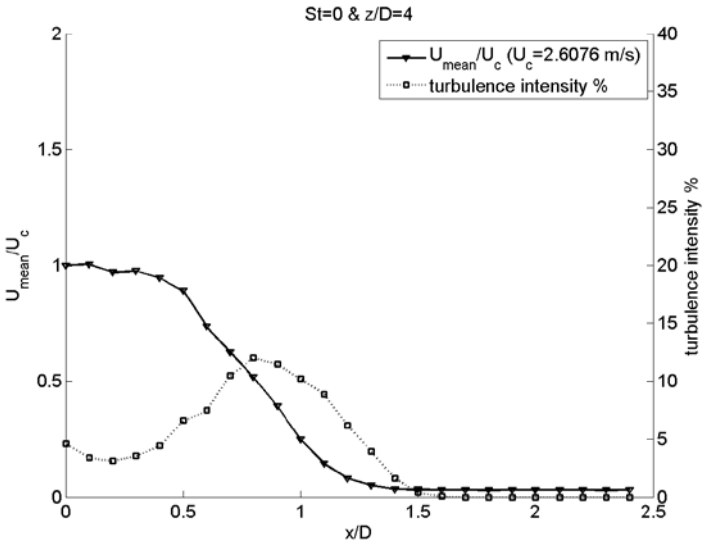

St=0.175

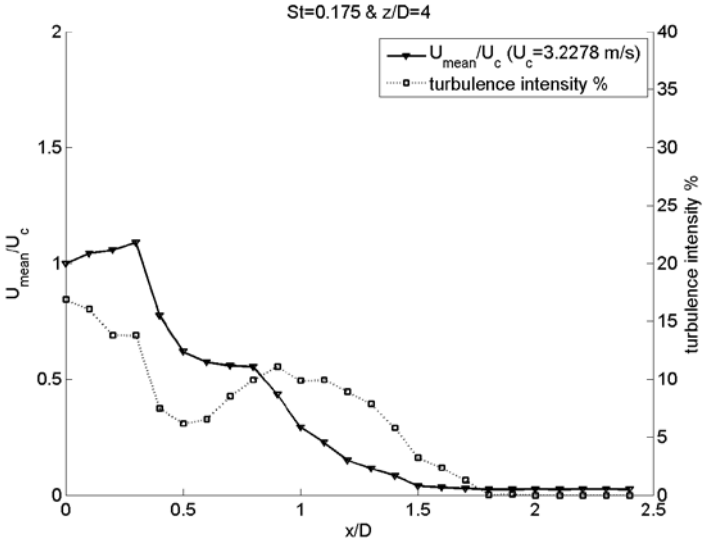

St=1

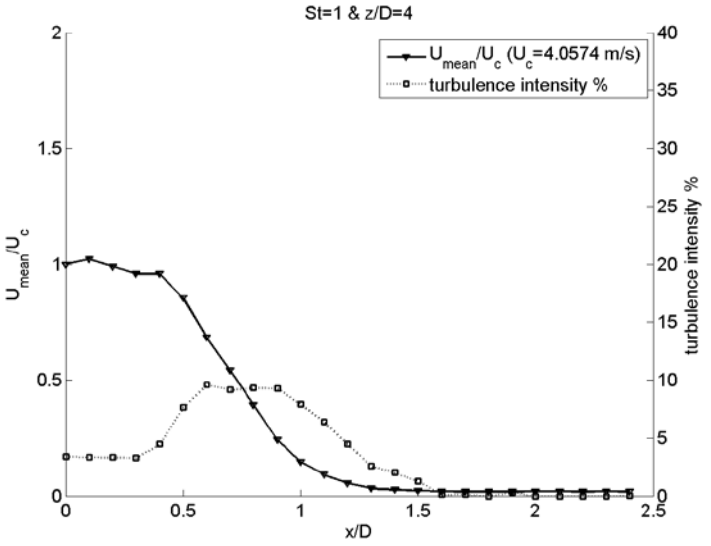

Figure 4.7. Normalized mean velocity and turbulence intensity plots for z/D=4

St=0

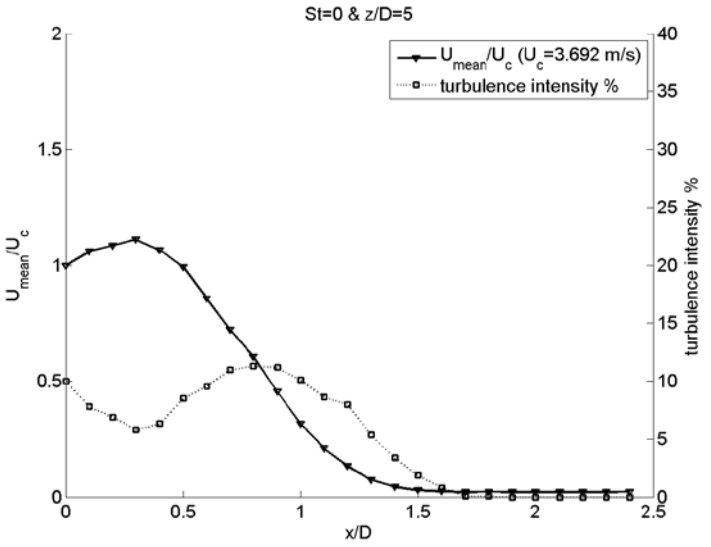

St=0.175

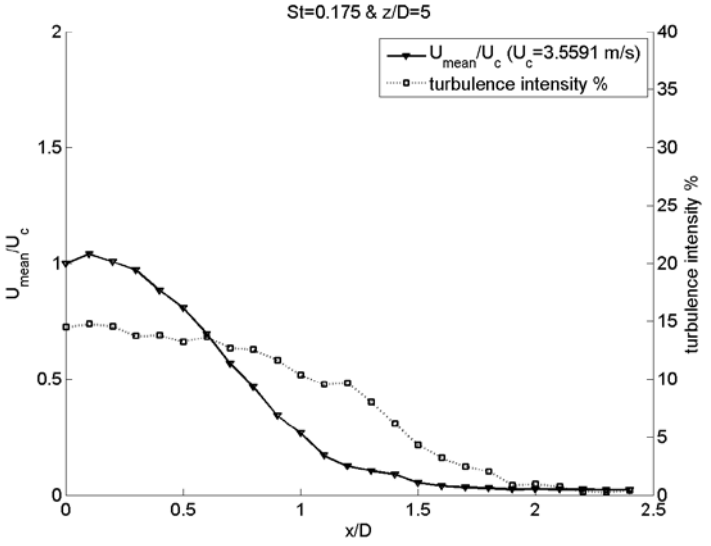

St=1

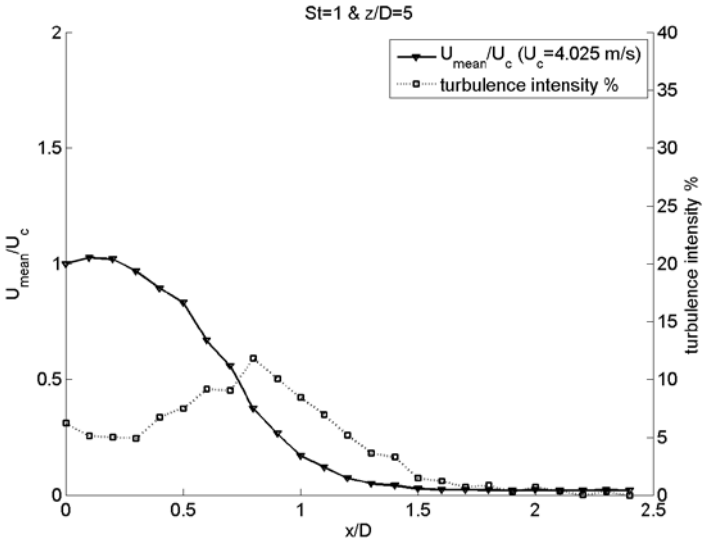

Figure 4.8. Normalized mean velocity and turbulence intensity plots for z/D=5

St=0

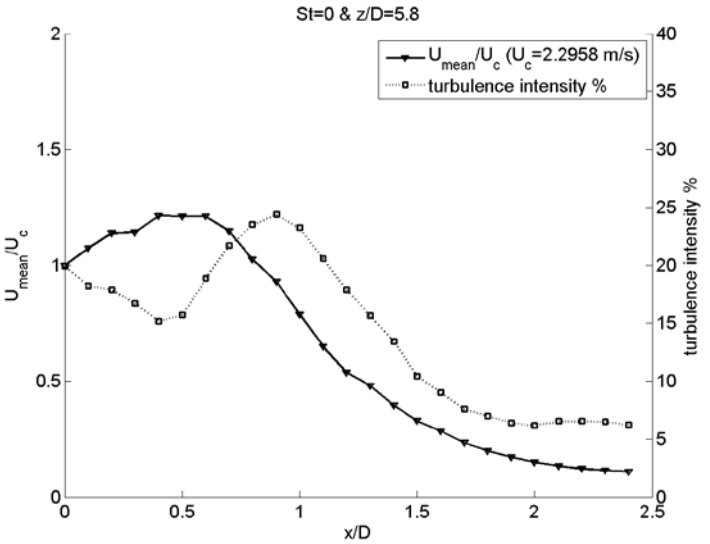

St=0.175

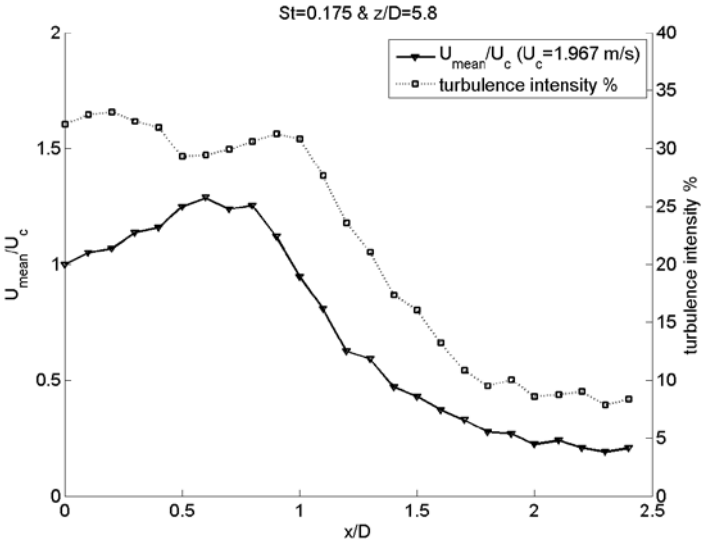

St=1

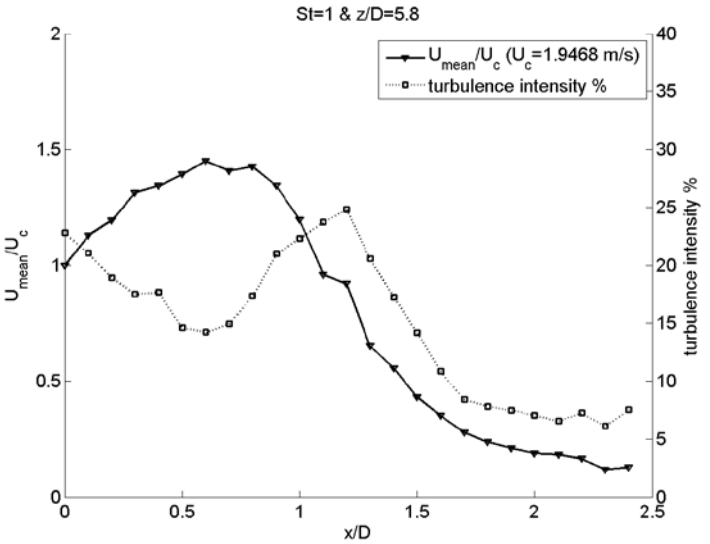

Figure 4.9. Normalized mean velocity and turbulence intensity plots for z/D=5.8

The velocity and turbulence intensity profiles at wall-jet region are given in Figure 4.10. Two noteworthy evidences are observed from these plots; First finding is the maxima of the turbulence intensity at very close to the jet centerline (x/D=0.5). Aforesaid location is where the jet flow has changed its direction suddenly that causes sharp turns in streamlines. It is thought that turbulence values have increased due to pressure change at that location. There is also peaks in velocity profiles at x/D=0.5 which is thought to be due to rapid acceleration of jet. This occurrence is also agreed with conclusions of Fairweather and Hargrave (2002).

Another interesting formation is that, a sudden decrease in turbulence intensity approximately from 15% to 7.5% at x/D=2.5 radial location. This sudden decrease is observed for all Strouhal numbers. This drop may also be due to a mechanical imperfection of the traversing mechanism.

St=0

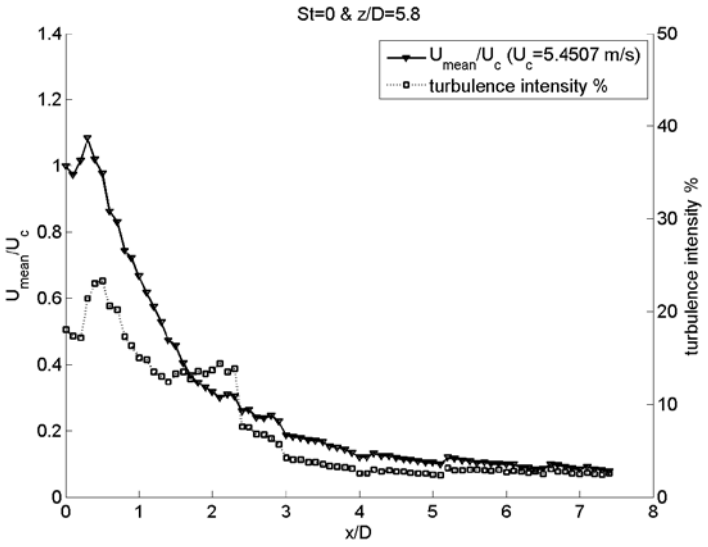

St=0.175

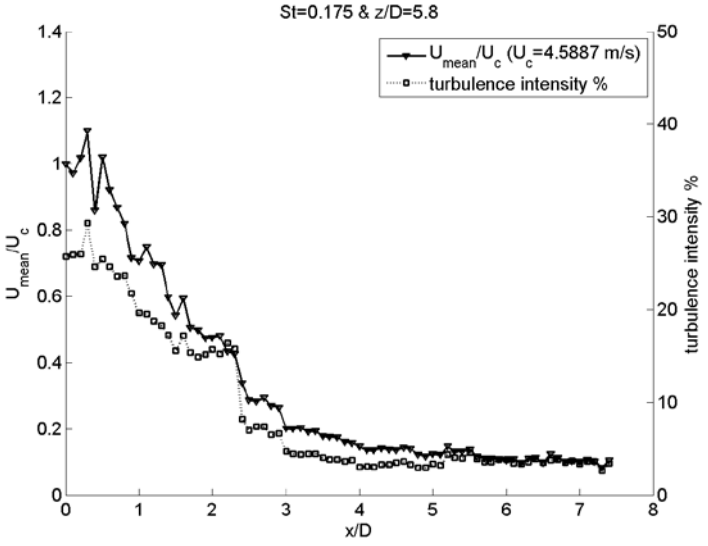

St=1

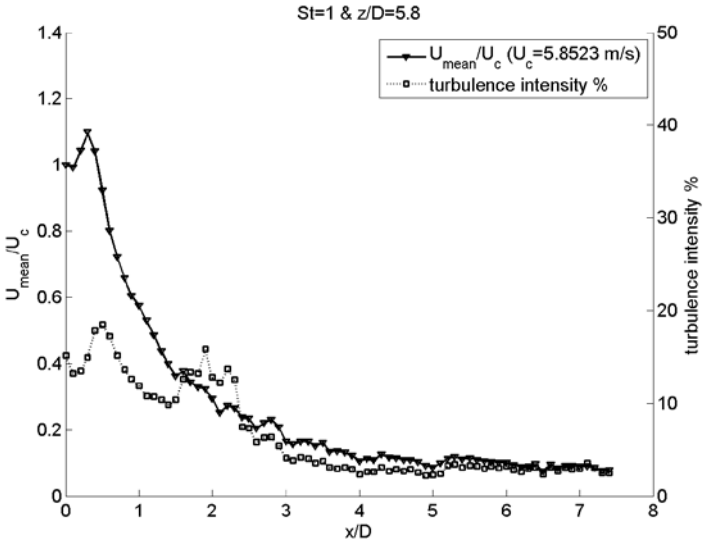

Figure 4.10. Normalized mean velocity and turbulence intensity plots for wall jet region

4.3. Effects of Turbulence Intensity on Nusselt number

For three different actuation cases, radial distribution of Nusselt number and turbulence intensity are plotted in Figure 4.11. An interesting formation was observed when these plots were examined. The turbulence intensity maximums at locations of x/D~0.5 and x/D~2.5 have a mixed effect on Nusselt number. In the high turbulence region near to the stagnation point, Nusselt number was also high, for all Strouhal values. However, Nusselt number was measured low in the high turbulence level region at x/D~2.5, which is an unexpected finding. A sharp drop on turbulence intensity has been observed at x/D=2.5. It is thought that, the reason of this drop is a change on flow regime (turbulent flow →transient flow) due to characteristic of flow or an error due to a mechanical imperfection of the traversing mechanism. The flow visualization studies show that semi periodic vortex structures exist in wall jet zone about the radial location of x/D~2.5. It is thought that these vortex structures circulate the hot fluid and eventually cause it to interact with the thermal boundary layer of wall. This interaction results in a negative effect on cooling of the wall at this location, although the turbulence intensity is high. Low Nusselt number is thought to be due to the wall jet separation, but there is no detailed flow visualization data to enlighten this occurrence.

St=0

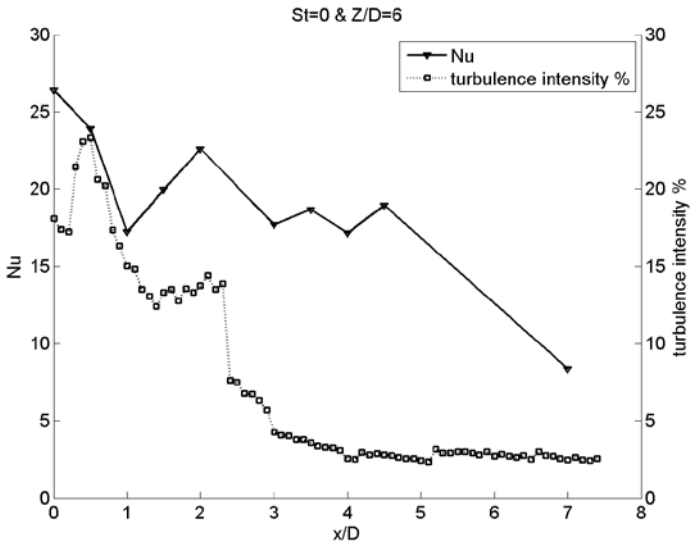

St=0.175

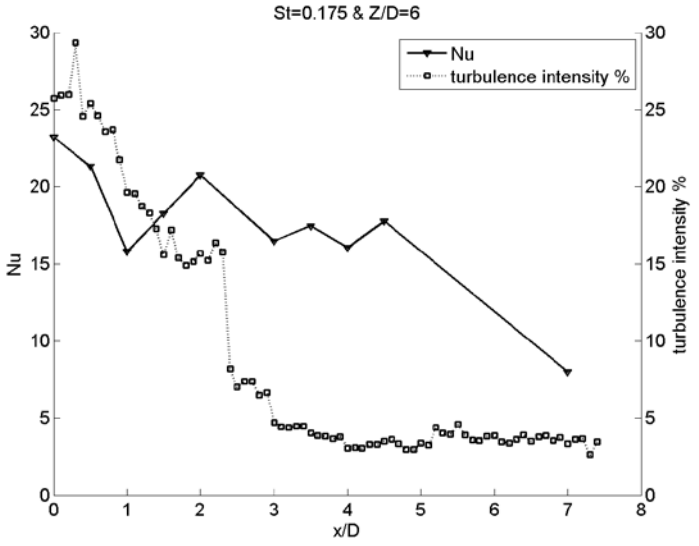

St=1

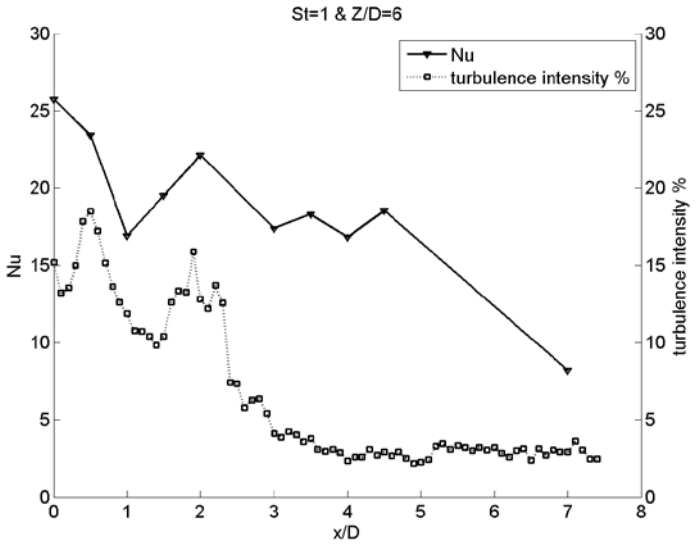

Figure 4.11. Effect of turbulence intensity on Nu number

4.4. Comparison with Earlier Studies

The results of present study are compared with earlier studies that were mentioned in the literature survey.

In Figure 4.12 and Figure 4.13, the results of Hwang and Cho (2003) (Re=34000 and Z/D=4) and present study is shown for cases which are St=0 and 1, respectively. It is obvious that, the main difference between turbulence intensity plots is that, their intensity values start from zero and increase in radial direction, whereas present results start from around 15% and have a peak at x/D=0.5, then decrease in radial direction. The Strouhal number has a decreasing effect on turbulence intensities, for present study. Nusselt number profiles show that, acoustic excitation has no significant effect on heat transfer.

Figure 4.14 shows the results of Baydar and Ozmen (2006) (Re=30000) and present study. Their turbulence intensity values start around 4% at stagnation point and increase up to 8% at the radial location of x/D~1. However, present results start around 15%. Their results also show that beyond x/D=3 radial location, trends on turbulence profiles similar between nozzle-to-plate spacing 1 and 6. It can be understood from Nusselt number plots that, for their study the heat transfer rates smoothly decrease whereas present results tends to fluctuate.

Figure 4.15 shows that the result of Roux et al. (2011) (Re=28000 and Z/D=5) and present study. Except the turbulence intensity values are lower than present study, the most similar profile to the present results is theirs.

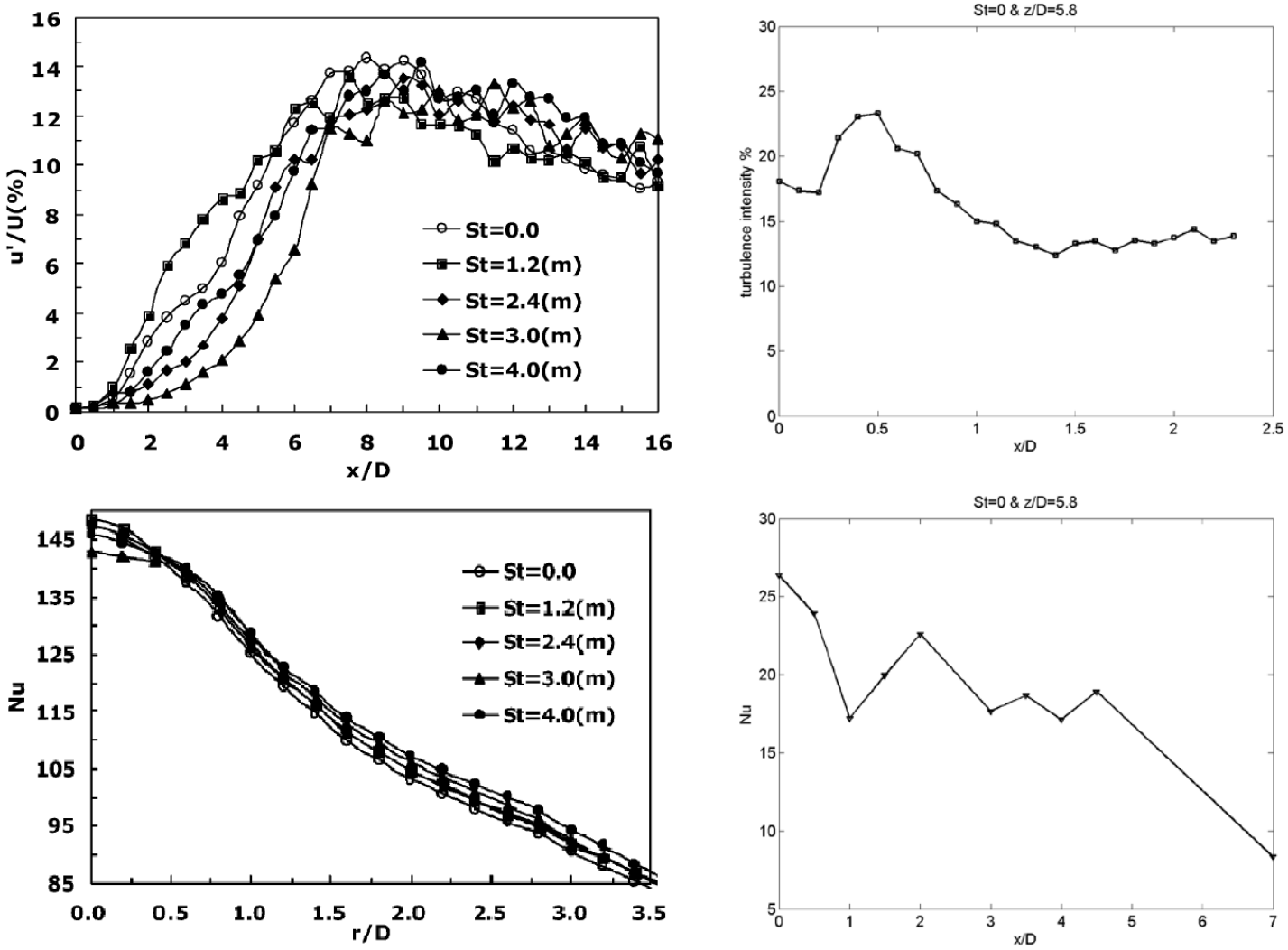

Figure 4.12. Comparison of Hwang and Cho (2003) and present study for St=0

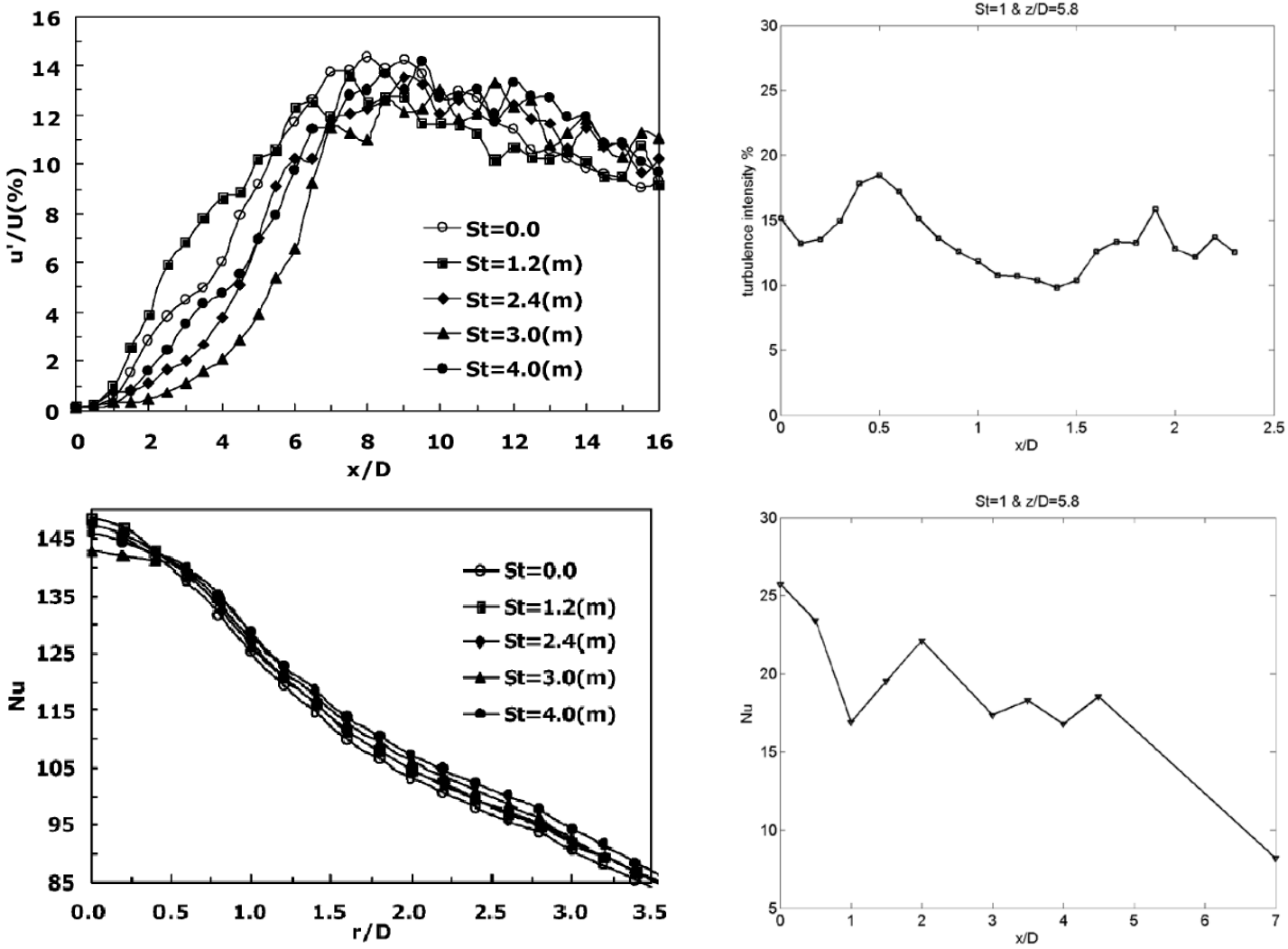

Figure 4.13. Comparison of Hwang and Cho (2003) and present study for St=1

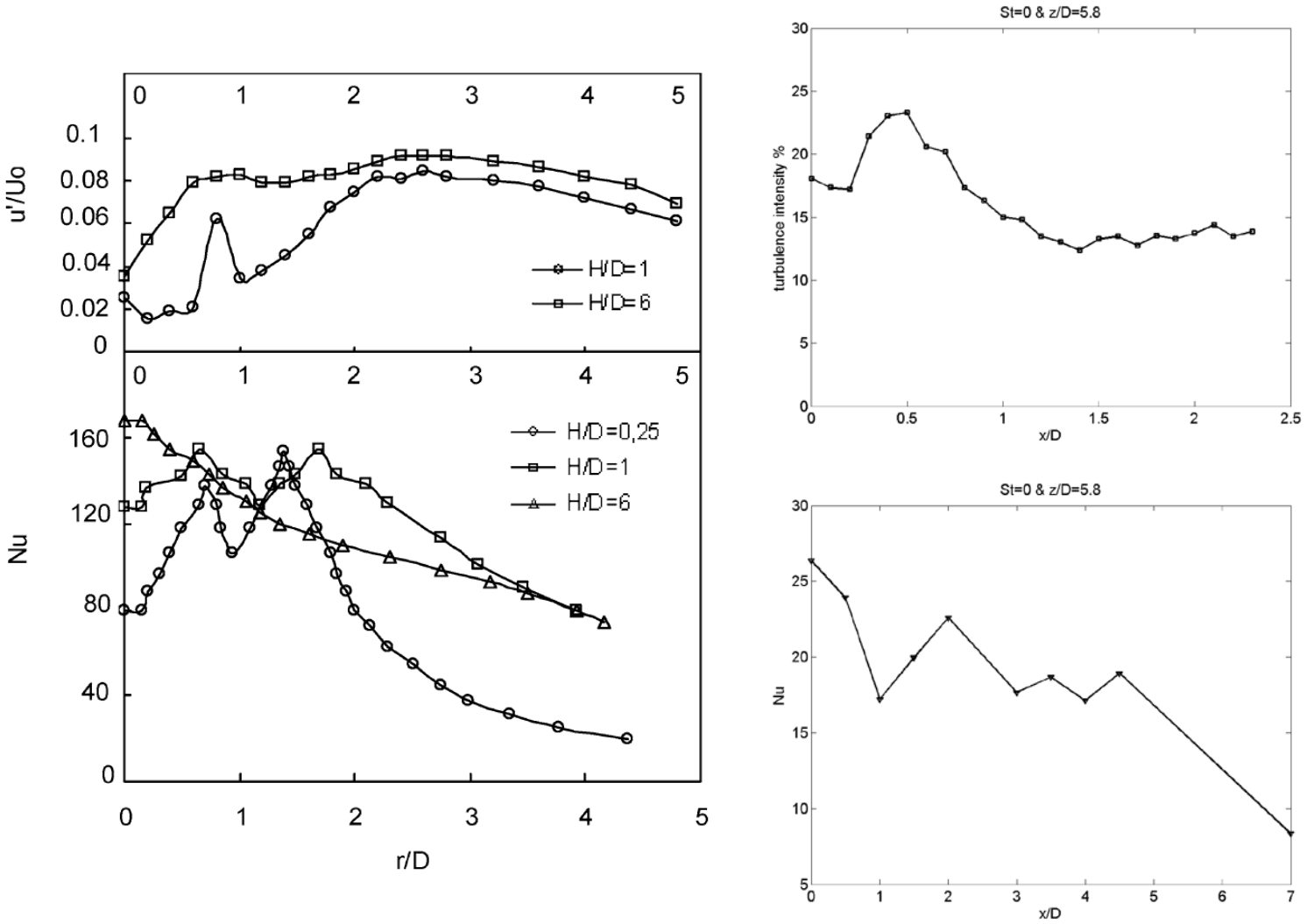

Figure 4.14. Comparison with Baydar and Ozmen (2006) and present study

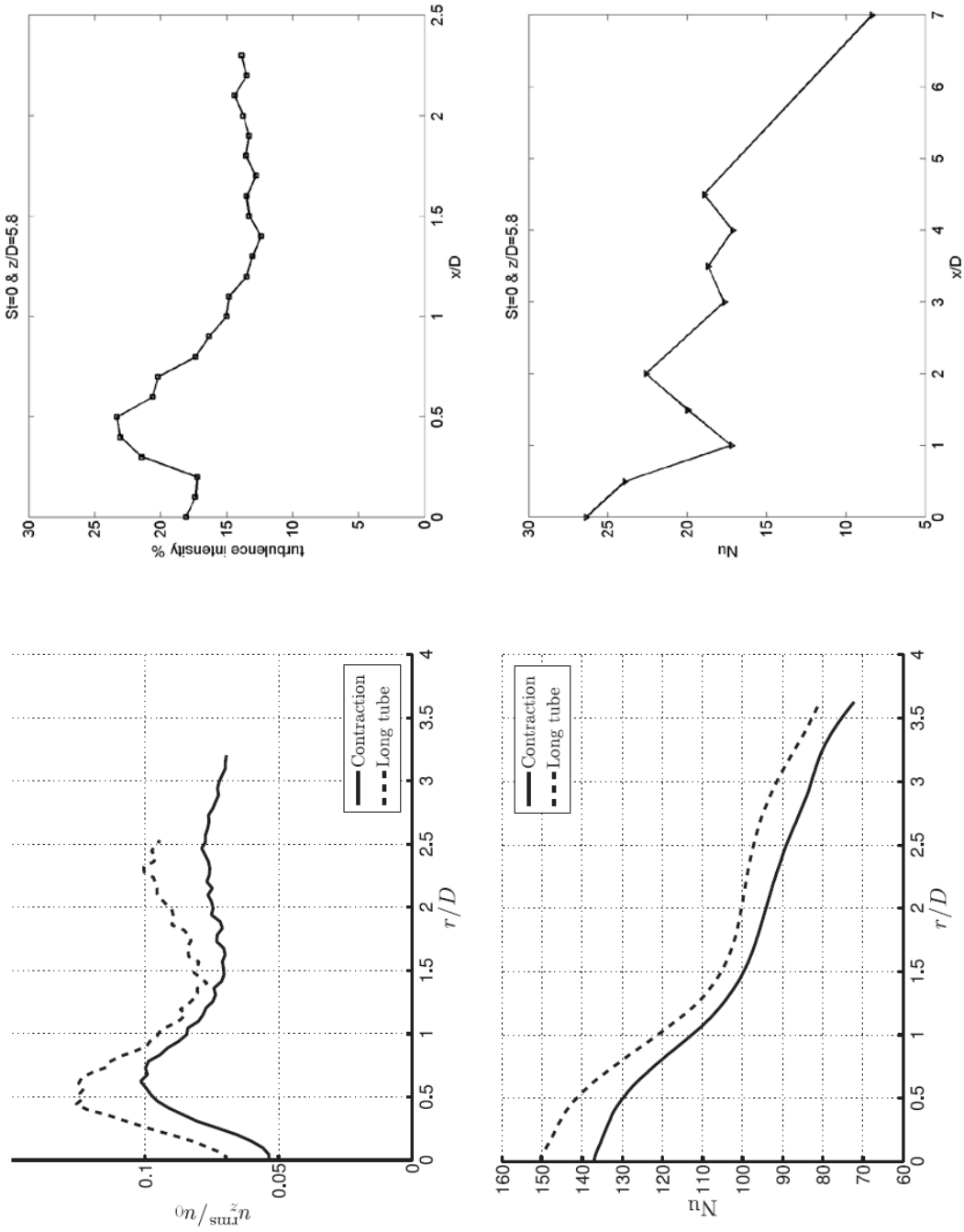

Figure 4.15. Comparison with Roux et al. (2011) and present study

CHAPTER 5

CONCLUSIONS

Velocity and turbulence measurement experiments in the wall jet region of an impinging round jet were performed in the scope of this work study. The aim of study is to have an idea about how the turbulence affects the heat transfer on impingement plate and how turbulence is influenced from acoustic actuation. Reynolds number is kept at 10000 for all experiments. Dimensionless nozzle-to-plate spacing is also constant which is six diameters. Strouhal number, which is dimensionless form of acoustic frequency, has three different values: 0 (no actuation case), 0.175 and 1.

Strouhal number is found to be effective in flow structure. As jet is actuated by increasing Strouhal numbers, width of the jet also increased in axial direction from nozzle exit to impingement plate. The turbulence intensities is measured high for the case of St=0.175 compared to the other cases. The roll-up events is observed for St=0.175 at location where is from 4 diameters downstream of nozzle exit. It is thought that, frequency related to the St=0.175 creates a special unsteady situation for jet flow. Effects of turbulence intensity on heat transfer are found to be interesting. Heat transfer rates obeyed the peaks in turbulence near the jet centerline; however, secondary peaks observed in turbulence have a counter effect on heat transfer. This is thought to be related very special geometry of test section, which is given in Figure 2.1, by differs from literature.

Finally, some recommendations might be helpful for better understanding the jet impingement phenomena to the researchers of future. They may be enlisted as follows:

- Velocity and turbulence measurements should be performed using direction sensitive probes such as x-wires.
- Velocity and turbulence measurements should be performed in wider range in radial direction.
- Optical measurement technics both flow characteristics and heat transfer rates could be performed to validation of this study.
- Pressure measurements should be performed to understand effects pressure distribution on impingement plate to jet flow.

REFERENCES

Baydar, E., and Y. Ozmen. "An Experimental Investigation on Flow Structures of Confined and Unconfined Impinging Air Jets." *Heat and Mass Transfer* 42, no. 4 (2006): 338-346.

Bilgin, N. "Experimental Investigation of Heat and Fluid Flow in an Actuated Impinging Jet Flow." M.Sc. Thesis, İzmir Institute of Technology, 2009.

Comte-Bellot, G. "Hot-Wire Anemometry." *Annual Review of Fluid Mechanics* 8, no. 1 (1976): 209-231.

Den Ouden, C., and C. J. Hoogendoorn. "Local Convective Heat Transfer Coefficients for Jets Impinging on a Plate: Experiments Using a Liquid-Crystal Technique." In *Proc. 5th Int. Heat Transfer Conf.*, 5, 293-297. Japan, 1974.

Fairweather, M. Fairweather, and G. Hargrave Hargrave. "Experimental Investigation of an Axisymmetric, Impinging Turbulent Jet. 1. Velocity Field." *Experiments in Fluids* 33, no. 3 (2002): 464-471.

Franco, G. "Boiling Heat Transfer During Cooling of a Hot Moving Steel Plate by Multiple Top Jets." M.Sc. Thesis, University of British Columbia, 2008.

Gardon, R., and J. C. Akfirat. "The Role of Turbulence in Determining the Heat-Transfer Characteristics of Impinging Jets." *International Journal of Heat and Mass Transfer* 8, no. 10 (1965): 1261-1272.

Gardon, R., and J. Carbonpue. "Heat Transfer between a Flat Plate and Jets of Air Impinging on It." In *Int. Developments in Heat Transfer*, 454-460. USA, 1962.

Hoogendoorn, C. J. "The Effect of Turbulence on Heat Transfer at a Stagnation Point." *International Journal of Heat and Mass Transfer* 20, no. 12 (1977): 1333-1338.

Hussain, A.K.M.F., and M.A.Z. Zaman. "Turbulence Suppression in Free Shear Flows by Controlled Excitation. ." *J. Fluid Mech.* 103, (1981): 133-159.

Jambunathan, K., E. Lai, M. A. Moss, and B. L. Button. "A Review of Heat Transfer Data for Single Circular Jet Impingement." *International Journal of Heat and Fluid Flow* 13, no. 2 (1992): 106-115.

Kline, S.J., and F.A. McClintock. "Describing Uncertainties in Single Sample Experiments." *Mech. Eng.*, (1953): 3-8.

Knowles, K., and M. Myszko. "Turbulence Measurements in Radial Wall-Jets." *Experimental Thermal and Fluid Science* 17, no. 1-2 (1998): 71-78.

Launder, B. E., and W. Rodi. "The Turbulent Wall Jet." *Progress in Aerospace Sciences* 19, no. 0 (1979): 81-128.

Martin, H. "Heat and Mass Transfer between Impinging Gas Jets and Solid Surfaces." *J. Matter. Process. Technol.* 136, no. 1-3 (1977): 1-60.

O'Donovan, T. S., and D.B. Murray. "Jet Impingement Heat Transfer – Part I: Mean and Root-Mean-Square Heat Transfer and Velocity Distributions." *International Journal of Heat and Mass Transfer* 50, no. 17-18 (2007): 3291-3301.

Obot, N.Y., A. S. Mujumdar, and W.J.M. Douglas. "Effect of Semi-Confinement on Impingement Heat Transfer." In *Proc. 7th Int. Heat Transfer Conference*, 3. Germany, 1982.

Popiel, C. O., and O. Trass. "The Effect of Ordered Structure of Turbulence on Momentum, Heat, and Mass Transfer of Impinging Round Jets." In *7th Int. Heat Transfer Conf.*, 141-146. Munich, Germany, 1982.

Raman, G., M.A.Z. Zaman, and E.J. Rice. "Initial Turbulence Effect on Jet Evolution with and without Tonal Excitation." *Physics of Fluids A* 1, no. 7 (1989): 1240-1248.

Schlichting, H. *Boundary-Layer Theory*: McGraw-Hill, 1968.

Schlunder, E.U., and V. Gnielinski. "Heat and Mass Transfer between Surfaces and Impinging Jets." *Chem. Ing. Tech.* 39, (1967): 578-584.

Tani, I, and Y Komatsu. "Impingement of a Round Jet on a Flat Surface." In *Proceedings of the 11th International Congress of Applied Mechnanics*, 672-676. New York: Springer-Verlag, 1966.

Wiltse, J., and A. Glezer. "Direct Excitation of Small-Scale Motions in Free Shear Flows." *Physics of Fluids* 10, (1998): 2026-2036.

Wolf, D. H., F. P. Incropera, and R. Viskanta. "Jet Impingement Boiling." In *Advances in Heat Transfer*, edited by P. Hartnett James and F. Irvine Thomas, Volume 23, 1-132: Elsevier, 1993.

Zuckerman, N., and N. Lior. "Jet Impingement Heat Transfer: Physics, Correlations, and Numerical Modeling." In *Advances in Heat Transfer*, edited by James P. Hartnett† Avram Bar-Cohen George A. Greene and I. Cho Young, Volume 39, 565-631: Elsevier, 2006.

Zuckerman, N., and N. Lior. "Impingement Heat Transfer: Correlations and Numerical Modeling." *Journal of Heat Transfer* 127, no. 5 (2005): 544-552.